PRIMER

Surface-enhanced Raman spectroscopy

Xiao Xia Han[1] ✉, *Rebeca S. Rodriguez*[2], *Christy L. Haynes*[2] ✉, *Yukihiro Ozaki*[3] ✉ *and Bing Zhao*[1] ✉

Abstract | Surface-enhanced Raman spectroscopy (SERS) is a highly sensitive technique that enhances the Raman scattering of molecules supported by some nanostructured materials. SERS allows for the structural fingerprinting of low-concentration analytes through the plasmon-mediated amplification of electrical fields or chemical enhancement. Owing to its ultra-high sensitivity and selectivity, SERS has a vast array of applications in surface and interface chemistry, catalysis, nanotechnology, biology, biomedicine, food science, environmental analysis and other areas. This Primer aims to provide interdisciplinary readers with key points regarding SERS methods. We briefly introduce the basic theories of SERS enhancement mechanisms. Details about SERS equipment, SERS-active material preparation and SERS measurements are summarized, followed by results and typical methods for data analysis. Recent applications of SERS in multiple research fields are then highlighted, including probing surface reactions and interfacial charge transfer, structural characterization and chemical/biological sensing. Furthermore, spectral reproducibility, SERS technical limitations and possible optimizations are discussed to provide readers with methodological guidance for the rational design of related studies. The Primer ends with a discussion of promising opportunities for SERS-based research in the future.

Surface-enhanced Raman scattering
The Raman scattering of a molecule is significantly enhanced when the molecule is either attached to or in proximity to a nanostructured surface.

[1]*State Key Laboratory of Supramolecular Structure and Materials, College of Chemistry, Jilin University, Changchun, China.*

[2]*Department of Chemistry, University of Minnesota, Minneapolis, MN, USA.*

[3]*Department of Biomedical Sciences, School of Biological and Environmental Sciences, Kwansei Gakuin University, Sanda, Hyogo, Japan.*

✉*e-mail:* *hanxiaoxia@jlu.edu.cn*; *chaynes@umn.edu*; *yukiz89016@gmail.com*; *zhaobing@jlu.edu.cn*

https://doi.org/10.1038/s43586-021-00083-6

Raman scattering, a form of inelastic scattering, originates from a shift in the energy of laser photons after light–molecule interactions[1]. Raman spectroscopy is useful for fingerprinting the structural information of molecules. Low sensitivity due to very weak Raman scattering is, however, a major issue associated with this spectroscopic technique[2]. A significant enhancement in Raman signal intensity can be achieved via surface-enhanced Raman scattering (FIG. 1a). Popular nanostructured materials such as nanoparticles (NPs), roughened films or nano-patterned substrates, enhance the Raman signals of analytes through surface plasmon enhancement or by chemical contributions[3]. Surface-enhanced Raman spectroscopy (SERS) allows for rapid, non-invasive in situ detection of target molecules[4–6]. Combined with the molecular resonance Raman effect, surface-enhanced resonance Raman scattering (SERRS) has gained increasing interest owing to its ultra-high sensitivity and selectivity. Meanwhile, developments in SERS theories, SERS-active materials (also referred to as SERS substrates) and related instrumentation have advanced a variety of applications in surface and interface chemistry, catalysis, nanotechnology, biology, biomedicine, food science, environmental analysis and other areas.

The underlying mechanisms of Raman scattering enhancement based on electromagnetic and chemical theories were proposed after the first observation of SERS on a roughened silver electrode[7–9]. Although there were several decades of debate about how the enhancement mechanisms work, two primary theories have thus far been well-accepted. Surface plasmons have been confirmed to play a crucial role in SERS[10–12]. When incident light strikes particles much smaller than the incident wavelength, localized surface plasmons are excited[13]. The frequency of the induced oscillation against the restoring force between the electrons and nuclei is determined by the inherent properties of the particle, such as its size, shape and morphology[14]. A localized surface plasmon resonance (LSPR) occurs when the light frequency matches the oscillation frequency of the electrons, inducing an enhanced electrical field near the particle surface[15] (FIG. 1b). This results in enhanced Raman scattering of adsorbates within that electromagnetic field. A metallic nanotip with an LSPR in the visible or near-infrared range is capable of exciting Raman scattering from a sample with a nanoscopic volume placed under the tip[16], a technique known as tip-enhanced Raman spectroscopy (TERS).

Chemical contributions to SERS are particularly important for those materials with a surface plasmon resonant absorption far away from commonly used laser excitation wavelengths[17]. Charge transfer (CT) is believed to contribute to SERS according to the chemical enhancement theory[18,19]. By contrast with enhancement of overall Raman bands based on the electromagnetic mechanism, selective enhancements of Raman bands are detectable owing to the CT contribution. The direction

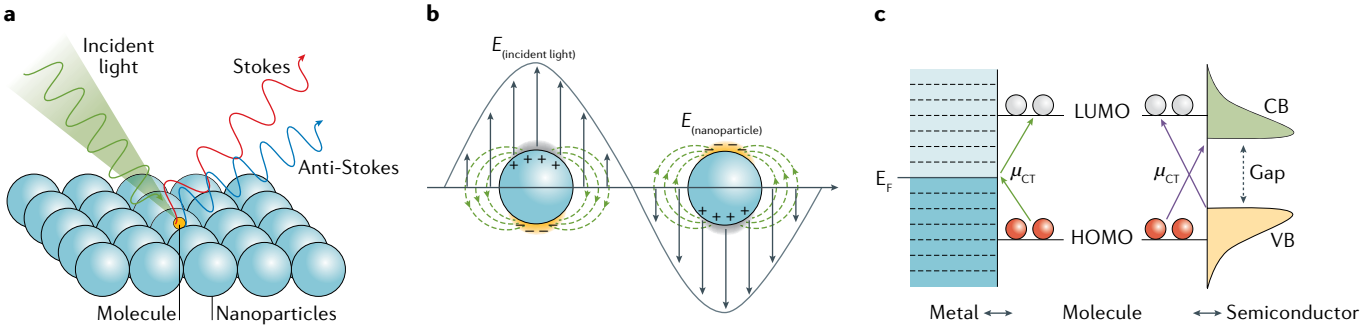

Fig. 1 | **SERS and its mechanisms. a** | Enhanced Raman scattering of a molecule adsorbed onto nanostructured particles resulting in emitted radiation with a lower (red) or higher (blue) frequency than the incident light, known as Stokes and anti-Stokes scattering, respectively. **b** | Localized surface plasmon resonance contribution to surface-enhanced Raman spectroscopy (SERS), electrical field (*E*); an enhanced electrical field on the metal surface allows Raman signal amplification. **c** | Charge transfer (CT) contribution to SERS at a metal–molecule or semiconductor–molecule interface; the CT transition (μ_{CT}) and arrows (green: metal–molecule; purple: semiconductor–molecule) show the CT directions. Red and white circles represent molecular orbitals. CB, conduction band; E_F, Fermi level; HOMO, highest occupied molecular orbital; LUMO, lowest unoccupied molecular orbital; VB, valence band.

of the CT transition (μ_{CT}) is highly dependent on the material, molecule and laser energy and can occur via a molecule-to-metal or metal-to-molecule pathway. When a molecule is adsorbed onto a metal surface, photo-induced electrons can be either excited from the highest occupied molecular orbital (HOMO) of the molecule and transferred to the Fermi level of the metal, or excited from the Fermi level of the metal and transferred to the lowest unoccupied molecular orbital (LUMO) of the molecule[20]. Semiconducting materials have an energy gap between their full valence band and empty conduction band, the energy levels of which may function like the Fermi level of plasmonic NPs in CT processes[21,22] (FIG. 1c). The two mechanisms are generally not mutually exclusive but contribute together to overall SERS signals. In a metal–semiconductor heterostructure, synergistic contribution of plasmons and CT can induce unprecedented SERS signals[23].

This Primer describes how Raman spectrometers are used for SERS measurements and discusses the fabrication of SERS-active materials. Methods for qualitative and quantitative analysis of SERS results are highlighted, providing readers with useful information about data analysis and theoretical evidence. Advances in SERS applications are then reviewed with the latest examples specifically in chemistry, materials science and bioscience. Additionally, spectral reproducibility and key optimization factors are discussed to promote the acquisition of strong and reproducible SERS signals, followed by a summary of technical limitations, current challenges and perspectives for future research.

Experimentation

In this section, we discuss the overall equipment, instrumentation and set-up needed to perform SERS experiments. Additionally, SERS requires the use of SERS-active materials, and so the most common of these are discussed, along with some of their advantages and disadvantages. Furthermore, as the use of SERS evolves, the requirements for different applications may advance to achieve better sensitivity. For this reason, we have also highlighted specialized SERS experiments that require specific set-ups or equipment.

Surface plasmons
A collective oscillation of conduction band electrons at the interface of two materials that occurs upon stimulation by incident light.

Equipment

Depending on the range of frequencies that are desired for a specific SERS application, there are a wide variety of laser sources that can be employed in a SERS set-up, ranging from the UV to the near-infrared. The continuous wave laser source excites the LSPR, and a notch or long-pass filter is used to reflect or absorb Rayleigh scattering so that the small number of Raman-scattered photons are detectable[24]. Other common optical components include interference filters to clean up the excitation beam and dispersive etched gratings to increase spectral resolution or photon collection efficiency[25]. For SERRS, it is important to have a laser excitation wavelength that is relevant for the molecular resonance of interest. Traditionally, this has been accomplished with a tunable laser, such as a dye laser. As lasers become less expensive, researchers instead purchase multiple diode lasers chosen to excite specific resonances of interest. A basic Raman spectroscopy set-up and three types of optical configuration are shown in FIG. 2a,b.

Most modern SERS instruments use charge-coupled device (CCD) detectors in which the spectral range varies based on the characteristics of the CCD chip used[26]. In cases where near-infrared excitation is used, InGaAs photodiode array detectors are used in place of silicon-based CCDs. There have also been strides to have SERS applicable in the deep UV (DUV-SERS) for a higher signal to noise ratio (SNR) in the detection of select aromatic compounds. This requires the use of a CT mechanism between semiconducting materials[27]. Details about these SERS techniques are summarized in TABLE 1.

SERS set-ups are easily amenable to the addition of cameras or microscope attachments to the original set-up to facilitate additional characterization, usually in the case of biological samples[28]. Most imaging with these microscopes falls into one of two categories: direct imaging[29] or hyperspectral imaging[30]. Direct imaging involves scanning the entire sample to obtain spectral information for a sample area over a small range of frequencies. Hyperspectral imaging — the more common approach of the two — acquires thousands of spectra from the sample in view and can be used to create images or maps indicating SERS intensity at specific

Raman-scattered energies in each scanned pixel. Like all traditional optical microscopes, these measurements are diffraction limited; the wavelength of light and the aperture characteristics determine the spatial resolution. SERS microscopy is often used for biological sampling of live cells because there is no need to label or fix the cells before imaging and, with high enhancement factor substrates, these spectral analyses can be acquired much more quickly than with other methods[28].

As SERS techniques advance or are combined with other techniques, the instrumental set-up becomes more complicated. TERS, for example, relies on both SERS and a near-field scanning microscope with a metal tip[31,32]. When the tip approaches the surface of the substrate or sample, it resonates with the LSPR, increasing the Raman-scattering intensity from the sample and exciting SERS from a small, localized portion of the sample[33,34]. Thus, the TERS tip has a crucial role in the application of the technique. Scanning tunnelling microscopy metal tips and metallized atomic force microscopy tips are often used for TERS. The sharpness, chemical composition (gold or silver) and overall morphology of the tip directly affects the TERS enhancement because of the concentrated electromagnetic fields generated between the tip and the metal surface. Lasers are generally introduced from the bottom of the sample or from the top of the sample near the tip (FIG. 2c). The distance between the tip and substrate or sample must be precisely controlled so that the analyte of interest is within the intense electromagnetic fields generated upon excitation of the plasmonic tip[35]. Spectroscopic surface science studies have been made possible by the recent construction of ultra-high vacuum (UHV) TERS instruments[36,37].

Preparation of SERS-active materials

SERS relies on the use of nanomaterials or materials with nanoscale features that exhibit a LSPR. These can be nanoscale materials derived from noble metals, such as silver, gold, aluminium and copper, transition metals[38], or dielectric and semiconducting materials such as conductive and doped oxides[39,40]. We discuss the synthesis and preparation of these materials briefly, as there are many reviews that go into greater detail regarding optimization of these SERS-active materials for specific applications[10,41,42].

Metal nanoparticles. As the field of nanotechnology expands significantly, there has been a large increase in the development of metal NPs of different sizes, shapes, features and uniformity for SERS applications (FIG. 3a). NPs can be synthesized via chemical reduction, chemical replacement and various types of chemical or thermal decomposition. The simplest way to synthesize uniform metal NPs is through chemical reduction[43]. A metal precursor, such as chloroauric acid[44] or silver nitrate[45], is chemically reduced by a reductant such as sodium borohydride or sodium citrate to generate metal NPs. Both time and temperature have a role in size and structure of the particles, and a surfactant is often added to prevent aggregation of the particles or to drive growth to a non-spherical morphology. Other factors that control size and shape depend on the starting materials and their respective concentrations, the pH of the reaction and the type of surfactant present during the synthetic reaction[46]. Non-conventional stabilizers, such as biomolecular ligands and biopolymers on the surface of metal NPs added during synthesis can also stabilize and/or reduce aggregation in the NP solution

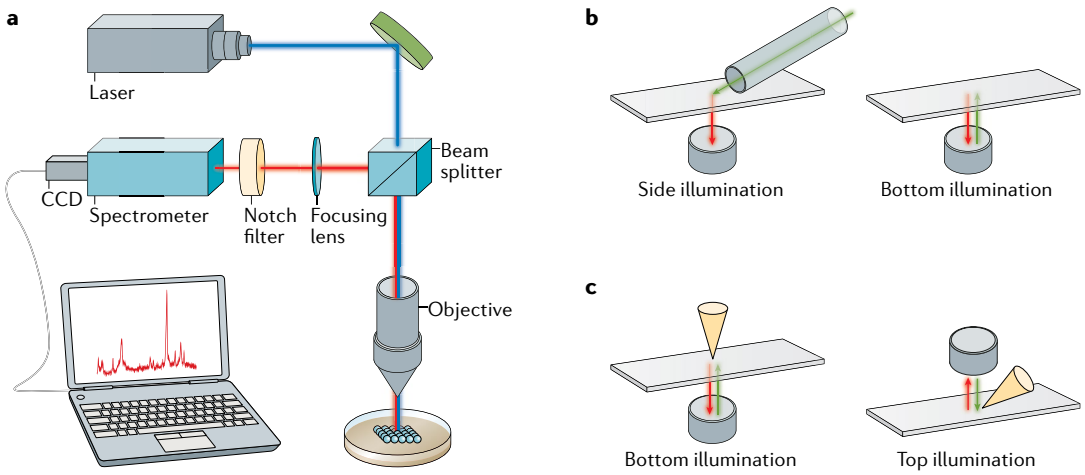

Fig. 2 | **Schematic of the Raman instrumental set-up. a** | A basic Raman spectroscopy set-up with a top illumination configuration. **b** | Two other illumination schemes common in surface-enhanced Raman scattering (SERS) experiments. On the left, side illumination from the top and scattered photon collection underneath. On the right, illumination and scattered photon collection underneath. **c** | Representative optical configurations for tip-enhanced Raman spectroscopy (TERS). On the left, illumination of the plasmonic tip and collection of scattered photons underneath the sample. On the right, illumination of the plasmonic tip and collection of scattered photons above the sample. CCD, charge-coupled device.

while providing a point of attachment for sensing applications[47]. Colloidal metal NPs come in many geometric shapes beyond spheres, such as spiky silver NPs[48], silver nanostars[49], gold nanowires[50], silver nanoflowers[51], gold nanorods[52] and gold nanosnowflakes[53], whereby their morphologies contribute to SERS performance. For example, spiky or pointed nanostructures may provide a large, focused enhancement or hot spot at the tip of these nanostructures, but tend to be less uniform overall, whereas nanorods or nanospheres may be more uniform, but comparatively less enhancing. Other noble metals, such as copper and aluminium, may be used to synthesize plasmonic metal NPs, but gold and silver are the most commonly used owing to their enhancement factors and stability[54]. Semiconducting nanomaterials have also been used as SERS-active substrates, relying on CT mechanisms[55]. Although colloidal plasmonic metal NPs are prevalent SERS materials, as they are synthetically tunable with large enhancement factors based on their refractive index properties, they often do not have a long shelf-life, which may be impractical for some SERS applications[56].

Film-over nanospheres. Metal film-over nanospheres are common, robust SERS-active substrates that are easily fabricated[57]. Briefly, they are defined as SERS substrates that have a nanoscale-thickness metal film covering self-assembled nanospheres (usually hundreds of nanometres in diameter) on a smooth substrate. These are one of the many possible solid film substrates and are made by drop-casting size-monodispersed nanospheres onto a flat substrate to achieve self-assembly on the surface, creating a monolayer or multilayer of closely packed nanospheres[58]. The flat substrates (for example, glass, mica or silicon) must be treated and cleaned with a piranha or aqua regia solution ahead of nanosphere assembly to ensure removal of organic or metal contamination that could disrupt the self-assembly. A plasmonic material, most often silver or gold, is then vapour deposited onto the surface of the substrate where the thickness and roughness of the metal has a direct correlation with the LSPR and the overall SERS enhancement. Although these substrates often vary in enhancement factor from batch to batch, they have a relatively long shelf-life and thus are practical choices for long-term SERS applications[59].

Lithographically defined nanostructures. There are various types of SERS-active substrate that are synthesized via lithography. These syntheses often use three different lithographic methods: nanosphere lithography, photolithography and electrochemical deposition lithography.

In nanosphere lithography, film-over nanospheres are synthesized as described above, and then the entire substrate is sonicated in an organic solvent to remove the self-assembled nanospheres after the metal is vapour deposited. This leaves behind ordered, nanoscale triangles in the voids between the previously closely packed nanospheres (FIG. 3b). Although this technique is relatively fast and inexpensive, the void pattern is limited by the self-assembly of the nanospheres, which may not always be perfect structures[46].

Photolithography has been used to synthesize SERS-active substrates; however, the spatial resolution of typical photolithography is insufficient for practical SERS applications for which one wants nanometre-scale control of the final structure[60]. Other lithographic techniques such as electron beam lithography[61] and focused ion beam lithography[62] use a focused beam to create seemingly perfectly patterned, highly ordered, metal nanostructures of various shapes, sizes and patterns. These island structures vary greatly from colloidal metal NPs because they do not need to be suspended in any medium or have surface-adsorbed reducing agents and/or surfactants, but also run the risk of degradation or oxidation without any protective coating on the surface. Additionally, electron beam lithography and focused ion beam lithography can be time-consuming and inefficient as both require each nanostructure to be made individually, generating only a limited SERS-active area on the substrate[63] (FIG. 3c). Evaluation of these structures can be accomplished with microscopy techniques and enhancement factor calculations.

Sample pretreatment and assembly

The largest enhancement of Raman signal is observed when the LSPR extinction maximum (λ_{max}), the laser excitation wavelength and the SERS scattering

Table 1 | **Equipment, applications and experimental considerations of SERS techniques**

Technique	Equipment	Application	Experimental considerations
SERS	Laser source, filters, detector, plasmonic substrate	Biological/chemical sensing, observation of chemical reactions and mechanisms, catalysis, electrochemistry	Plasmonic substrate, acceptable enhancement factor
SERRS	Tunable laser source, filters, detector, plasmonic substrate	Biomolecules, biological systems	Analyte absorption band needs to match laser wavelength
TERS	Near-field scanning microscope with a metal tip	Structure/morphology of 2D materials, single molecules, semiconducting nanostructures	Sharpness and morphology of metal tip highly affect the sensitivity
UV-SERS	UV excitation source, filters, detector, plasmonic substrate	Select biological and aromatic molecules	Plasmonic substrate must have enhancement in the UV range
DUV-SERS	DUV excitation source, filters, detector, plasmonic substrate	Biological molecules, select aromatic molecules, semiconducting materials	Molecules must have electronic resonances in the UV range

DUV, deep UV; SERRS, surface-enhanced resonance Raman spectroscopy; SERS, surface-enhanced Raman spectroscopy; TERS, tip-enhanced Raman spectroscopy.

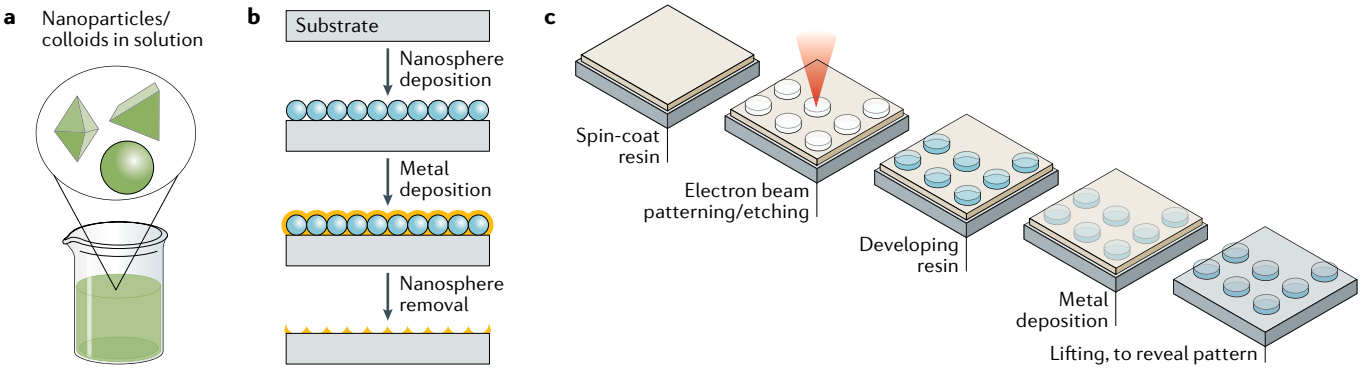

Fig. 3 | **Schematic of common surface-enhanced Raman spectroscopy nanostructure fabrication strategies.** **a** | Solution-phase colloidal nanoparticles with varied size and morphology depending on reactants and/or surfactants incorporated. **b** | Self-assembly-based lithography in which silica or polymer nanospheres are used as a template ahead of noble metal deposition[46]. **c** | Electron beam lithography in which nanostructure size and arrangement are fabricated in a serial fashion. Part **b** adapted with permission from REF.[46], ACS.

wavelength are well aligned[64]; NPs can be tuned to achieve this enhancement[13]. Although the size of NPs, metal thickness, nanostructure shape and spacing and refractive index of the substrate and surrounding medium all have a role in the LSPR extinction maximum of plasmonic substrates, organic surface contamination of the solid substrates may contribute to this as well[59]. Plasma cleaning with argon or other gases for short periods of time can be used to eliminate any contamination on the plasmonic surface[65]. In general, plasma cleaning shifts the LSPR to higher energies as the refractive index at the nanostructure surface decreases; this shift should be accounted for experimentally. Lengthy plasma treatment has the potential to damage the nanostructure, making the substrate unusable.

Although some target analytes can directly adhere to plasmonic NPs or plasmonic solid substrates, most SERS sensing requires the use of some type of attachment chemistry, an affinity agent or a SERS tag to sense the target. Intrinsic SERS is the direct sensing of the desired target, while extrinsic SERS relies on the use of some sort of SERS tag to indicate sensing of the target. Briefly, the target can be modified to exploit direct attachment to the SERS-active material through covalent bond chemistry, anionic and cationic interactions or weak van der Waals interactions. If that is not possible, the use of an affinity agent such as an aptamer, antibody, small molecule or polymer can be used to facilitate sensing through direct capture of the target[66,67]. Lastly, extrinsic SERS tags are plasmonic nanostructures functionalized with a ligand and Raman reporter that can readily bind specifically to the desired target. The tag is designed to yield a large SERS signal; however, any spectral changes observed yield only information about the tag rather than the vibrational modes inherent to the target itself. Both intrinsic and extrinsic SERS measurements have greatly advanced SERS sensing applications with trade-offs regarding the benefits to direct and indirect sensing[68,69]. Details and comparison of the SERS-based strategies are listed in TABLE 2.

When SERS spectra are collected, both the acquisition time and laser power play a part in the resulting data. It is important to note that too high a power — particularly in a small focal laser spot — or too long an acquisition time at a higher power can damage biological samples. SERS fingerprints of samples will suffer from significant alteration when the samples are damaged by the laser applied during the measurement. Laser power-dependent and acquisition time-dependent spectral collection is thus useful for experimental optimization. The choice of laser wavelengths depends on the purpose of a study. To obtain SERRS, a certain laser wavelength close to the electronic absorption of a chromophore of the target molecule is generally selected.

Dynamic measurements

Traditionally, performing fast dynamic measurements with SERS has been somewhat limited owing to two major factors: the inefficient nature of the inelastic scattering leading to long integration times and the variable enhancement across a substrate leading to substrate-induced spectral variation that obscures dynamic molecular information. Despite these limitations, there has been some progress towards using SERS for dynamic measurements. High-profile progress towards dynamic SERS measurements was first made in 1997 with the publication of two papers that demonstrated single-molecule SERS spectra for the first time[70,71]. Single-molecule SERS spectra are generally achieved by working with very low concentration dye molecules interacting with electromagnetic hot spots formed in agglomerating plasmonic colloids. One major component that proves single-molecule proof detection lies in the spectral dynamics, specifically in a Poisson distribution of SERS intensities as individual molecules move in and out of an electromagnetic hot spot. More recently, a process named dynamic SERS demonstrated the possibility of statistically accounting for spectral noise caused by Brownian motion of colloidal plasmonic NPs[72,73]. By subtracting this noise, it was possible to eliminate the overwhelming solvent background and reveal the relatively small signal of the SERS-active colloid-adsorbed molecules. The dynamic SERS technique was extended to demonstrate detection of analytes that were not strongly adsorbed, revealing rare events that are usually obscured in time-averaged spectra[74]. Finally, it has been shown that even when a substrate and adsorbed species appear relatively stable,

Table 2 | **Details and comparison of the three SERS-based strategies**

Strategy	Advantages	Disadvantages
Intrinsic SERS	High reliability and accuracy	Low sensitivity for molecules with low Raman cross-sections
Electrostatic binding	Good universality	Random orientation of molecules, possible disassociation and poor spectral reproducibility
Covalent binding	High stability	Specific groups such as thiols are necessary
π–π Stacking	Compatible with hydrophobic molecules	Low sensitivity
Combined SERS	Making inactive molecules active	Limited molecule types
Electrostatic–covalent binding	Making inactive molecules active	Limited molecule types
Extrinsic SERS	High sensitivity	Possible false positive results due to nonspecific binding
Electrostatic binding	Easily conducted	Relatively low accuracy
Covalent binding and exposed	Easily fabricated and stable binding	Susceptible to the environment, poor spectral reproducibility
Covalent binding and embedded	High stability and spectral reproducibility	Complicated synthetic procedures

SERS, surface-enhanced Raman spectroscopy.

there are significant dynamic SERS intensity fluctuations[75]; the source of these fluctuations is assumed to be time-dependent molecular rearrangements near SERS hot spots, but this is still under investigation.

In some cases, dynamic SERS has been achieved by designing SERS substrates that are physically dynamic, meaning that the particular solution conditions induce or disrupt plasmonic formations that facilitate the capture of SERS spectra. For example, assembly of a hydrogel structure with embedded plasmonic nanostructures yielded differing SERS enhancement factors at different water temperatures[76]. Responsive plasmonic structures hold significant potential for sensing applications; as such, various analyte-triggered responsive structures have been implemented including those that sense microRNA[77], small-molecule chemical messengers (such as H_2O_2)[78] and resonance Raman-active single molecules[79], among others.

As single NP or nanostructure SERS has become increasingly common, there has been increased interest in dynamic high-throughput measurements from many individual nanostructures or from a gradient of analyte concentrations. As such, various microfluidic platforms have been developed to dynamically perform SERS measurements as components move through the fluidic device[80]. SERS has been performed on both droplet[81] and continuous flow[82] microfluidic devices made from glass[83], polydimethylsiloxane (PDMS)[84] and paper[85] where the SERS nanostructure is the bottom of an assembled device[51], embedded in device walls[83] or introduced as a reagent[85].

In some cases, the type of dynamic information desired describes variation in spatial spectral signatures, and there has been significant progress to develop techniques whereby one can probe these variations. The most ubiquitous technique for spatially dynamic measurements is TERS, whereby plasmonic character is imbued to a tip that is scanned over the sample of interest[86]. The tips used include atomic force microscopy tips, scanning tunnelling microscopy tips, near-field scanning optical microscopy probes and nanopipettes[16,87]. Structural and plasmonic design of the probe tips remains a challenge for reproducible, high-spatial-resolution TERS; however, the method has already been employed to study a wide variety of systems including inorganic[88,89] and organic surfaces[90,91], surfaces undergoing chemical reactions[92,93] and live biological cells[94].

SERS imaging collection

Whereas TERS is a recent and exciting advance in SERS-based imaging, in part because it does not require the molecule or system of interest to adhere to or dwell very close to a plasmonic substrate, more traditional SERS imaging studies are performed regularly to investigate various chemical systems. SERS imaging can be accomplished either by probing molecules or very thin films adsorbed to a plasmonic Raman-enhancing substrate or by imaging a sample in which sites of interest are indicated by the presence of an extrinsic SERS label; the latter approach is much more common[95,96]. This application area has advanced significantly in the past two decades and includes various examples in which in vivo SERS imaging has been accomplished[97]. One particularly exciting development in SERS imaging is the application of super-resolution microscopy to achieve Raman vibrational information with sub-diffraction-limited spatial resolution[26,98,99].

Results

This section provides readers with an understanding of data processing and analysis, including data processing, band assignment, qualitative analysis, quantitative analysis, multivariate analysis and quantum chemical calculations.

Data processing

In data processing, it is important to consider the quality of SERS spectra; SNR and reproducibility of SERS spectra are particularly important. After collection, SERS data including the Raman wavenumbers and intensities are often transformed into ASCII format before being exported, to facilitate further data processing by software such as Origin. Details about the measurements, including the excitation wavelength, laser power at the sample, acquisition time and accumulation time, should also be stored. A control spectrum of the SERS substrate must also be stored for background subtraction. A high-intensity background originating from internal fluorescence in the raw data can be removed by baseline correction, which is particularly important for intensity comparison when managing multiple datasets. Spike removal and smoothing are usually useful to improve the spectral quality. For qualitative analysis, frequency shifts and selectively enhanced Raman bands should be of particular concern. Additionally, normalization of one band intensity is useful for comparing relative intensities in quantitative analysis. For calibration curves, multiple datasets should be stored and analysed to evaluate

batch-to-batch variation. The key points in the steps involved in SERS data analysis are shown in FIG. 4a.

Band assignment

Band assignment is always a key component of any kind of vibrational spectroscopy. The purpose of the band assignment is to understand with which kind of vibrational mode each band is concerned. The band assignment is essential for qualitative and quantitative analysis and molecular structural studies[1,2]. In a SERS experiment a molecule is always adsorbed onto a metal surface, and thus a SERS spectrum is somewhat different from the corresponding Raman spectrum. The band assignments in SERS spectra are almost the same as those in normal Raman spectra; however, some special precaution must be taken for the former as described later. Therefore, in this section the band assignments of normal Raman spectra are outlined first and, then, specific points for the SERS band assignments are explained.

Normal Raman spectra. Although there is no absolute procedure for assignments of Raman bands, several approaches have been effective. First, look for group frequencies such as the C=O, OH and C–S stretching modes and the CH_2 bending mode by comparing the frequency of an observed band with those frequencies assigned in the literature[100]. During the comparison, both intensities and frequencies must be noted. Obtained Raman spectra can also be compared with the spectra of entirely or partially similar molecules. The observed spectrum can also be compared with a Raman spectrum of a corresponding isotope-substituted molecule that contains deuterium, ^{15}N and/or ^{13}C. Spectra can be measured while varying the conditions (temperature, pH and solvent) of a molecule and, then, the obtained spectra are compared with each other to find out the spectral changes induced by the perturbation. Quantum chemical calculations can also be used, such as density functional theory (DFT) calculations.

Other methods of band assignment include measuring depolarized Raman spectra or using excitation wavelength-dependent Raman measurements. Band assignment can be done using reported bands in the literature, but care must be taken because previously published band assignments may not always be correct, or they may not be supported by solid evidence.

SERS spectra. A band shift may occur in a SERS spectrum[101–103]. For example, in the case of chemisorption a significant band shift due to CT may be observed[17]. There can also be large variation in Raman band intensity[3,104], whereby the intensity change depends on the

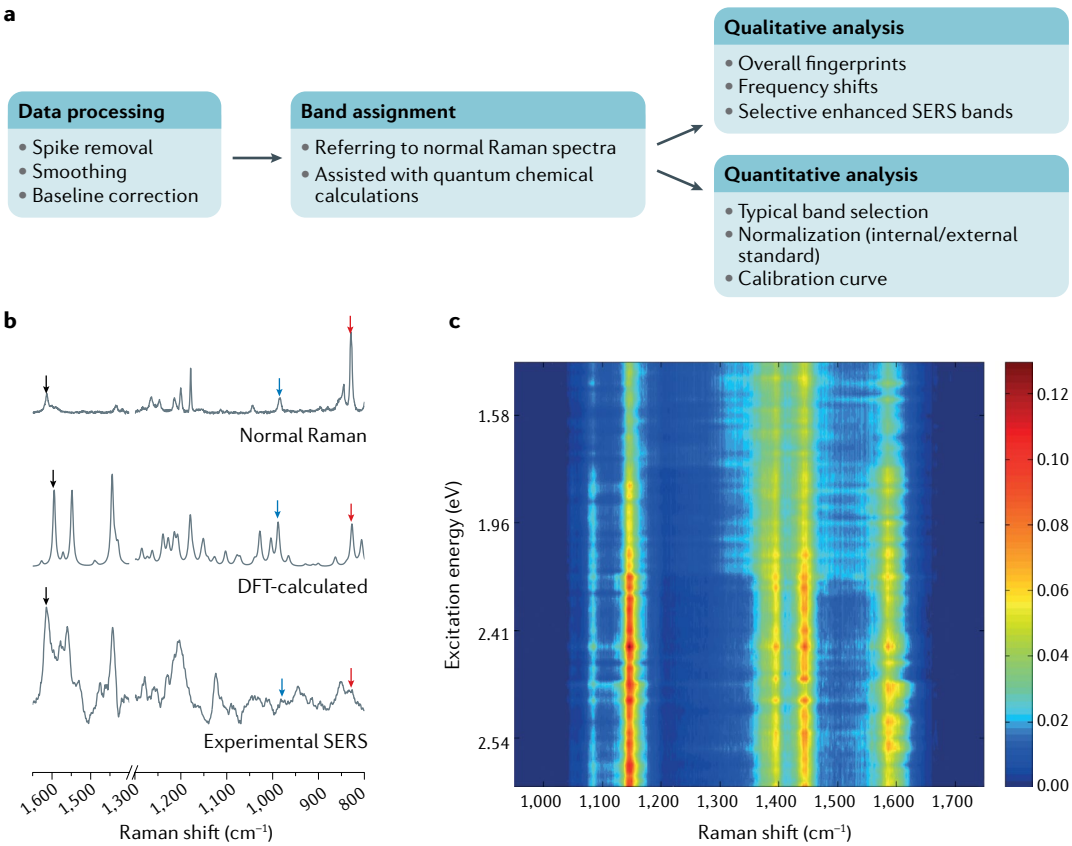

Fig. 4 | **SERS data analysis. a** | Steps involved in surface-enhanced Raman spectroscopy (SERS) data analysis include data processing, band assignment and qualitative and/or quantitative analysis. **b** | SERS band assignment for a peptide containing tyrosine, based on normal Raman spectra and density functional theory (DFT) calculation; the SERS bands of tyrosine are assigned based on the arrows marked with the same colour (red: ring breathing; blue: C–C stretching; black: N–H vibrations). **c** | Laser energy-dependent SERS spectral trajectory of PATP at a Cu–ZnO–PATP assembly. Part **b** adapted with permission from REF.[105], ACS. Part **c** adapted with permission from REF.[106], ACS.

CT resonance
The charge transfer (CT) contribution to surface-enhanced Raman spectroscopy reaches the maximum when the incident laser energy matches the CT excitation energy.

orientation of an adsorbed molecule and the distance from the metal surface. A part of a molecule that is in the close proximity to the SERS surface shows a stronger intensity enhancement in the spectra than other more distal parts of the molecule.

There are also selection rules for SERS. In electromagnetic enhancement, the intensity of a SERS band depends on the electrical field, the molecular orientation and the distance from the molecule to the material surface. In CT enhancement, CT resonance is crucial for selective Raman signal enhancement. For example, molecules that have nitrogen and sulfur atoms — which have lone pair electrons — produce SERS spectra with high intensity. A typical example for band assignment is shown in FIG. 4b, where the SERS bands of a tyrosine residue can be confirmed based on its normal Raman and DFT-calculated spectra[105].

Qualitative analysis

SERS is used extensively for various kinds of qualitative analysis because it demonstrates high selectivity as well as high sensitivity[101–104]. For qualitative analysis by SERS, high-quality SERS data with high reproducibility must be used. Proper pretreatments of experimental SERS data (FIG. 4a) are usually important. Trajectories of multiple SERS spectra are helpful for qualitative analysis of CT effect at ZnO–PATP interfaces[106] (FIG. 4c).

SERS is useful for the detection of spin states in a haem of myoglobin derivatives[107]. Owing to the enhancement order from the surface selection rule, SERRS spectra may give different conclusions in qualitative analysis compared with the resonance Raman spectra[107,108]. SERS is able to monitor cell cycle progression: a living human malignant cell line has been analysed using nuclear-targeted silver NPs modified with polymers, showing that SERS spectra were correlated with cell cycle phase progression recorded using dark-field imaging and flow cytometry[109]. Another interesting work used chemically synthesized highly symmetrical nanoporous silver microparticles to develop a 3D SERS imaging study of polymer blends[110]. The 3D patterns of the particles are very regular and predictable, resembling the particle shape and exhibiting symmetry. 3D SERS imaging has demonstrated a significant improvement in spatial resolution along the *z*-axis, which is a key point for Raman measurement in layered polymeric materials.

Quantitative analysis

For quantitative analysis by SERS, sensitivity and reproducibility of SERS measurements are two major important factors[3,101,104]. The stability of a SERS substrate is also a significant factor for SERS measurements. Therefore, to consider quantitative analysis by SERS, deep consideration about SERS substrates for high sensitivity, selectivity and stability are essentially important. Many quantitative analysis studies using SERS have been reported, some of which have been used for SERS sensors[3,101,104]. Chemometrics analysis such as partial least squares (PLS) regression is often used for quantitative analysis by SERS, but occasionally it is sufficient to use one single band.

In some cases the use of an internal or external intensity standard is effective in estimating relative intensity for quantitative analysis. The intensity of an internal standard may change on the basis of experimental conditions, such as the excitation wavelength used. Intensity may also vary upon the formation of an interaction between a part of the molecule that gives the internal standard and another molecule. Alternatively, the intensity of an external intensity may also vary by the interaction between the external molecule that gives the external standard and the analyte. Care must be taken in choosing the intensity standard. Before performing quantitative analysis, spectra pretreatments such as smoothing, baseline correction and a calculation of average spectra are usually necessary.

Multivariate analysis

Multivariate analysis is currently a popular approach for SERS spectral analysis (FIG. 5a); principal component analysis (PCA) allows relatively easy extraction of valuable information from complicated SERS spectra. PCA is often used for qualitative analysis (such as for classification, discrimination, cluster analysis) and imaging analysis, whereas PLS is used for quantitative analysis[101,102,104]. Multivariate curve resolution (MCR) is popular in imaging analysis and spectral analysis.

For SERS chemometrics analysis, spectra with poor SNR should be avoided. Proper data preprocessing such as noise deduction, baseline correction and averaging the spectra are required to obtain meaningful results.

Qualitative analysis and classification. PCA is a general method to separate and group samples on the basis of variance within SERS samples. PCA is powerful, but it is not always sufficient to distinguish closely related sample classes using their complex spectral profiles and, thus, supervised analysis is often applied as predictive models. Discriminant function analysis, which maximizes the within-group to between-group ratio to differentiate between classes, is popular among the supervised analysis methods. A dendrogram was developed on the basis of discriminant function analysis output using hierarchical cluster analysis (HCA) for a set of seven clinical isolates of *Escherichia coli* from a urinary tract infection[111]. The dendrogram based on a combination of PCA and HCA produced correct groupings including discrimination to strain level for a sample group of *E. coli*. PCA combined with linear discriminant analysis (LDA) has been used to separate label-free SERS spectra of blood samples from 49 patients with diabetes and those from 40 healthy volunteers[112]. There is also evidence of the potential of an orthogonal PLS discriminant analysis method in the label-free screening of cancers[113] (FIG. 5b).

Quantitative analysis by PLS regression. PLS regression has been used on the SERS spectra of serum and urine for the detection of chronic kidney disease in patients[114]. PCA combined with PLS regression has been useful for SERS-based biosensors[115]; SERS spectra were shown to be distinguishable by PCA even when manganese superoxide dismutase was at 10 pmol, and PLS regression was able to predict protein concentrations within one order of magnitude (FIG. 5c).

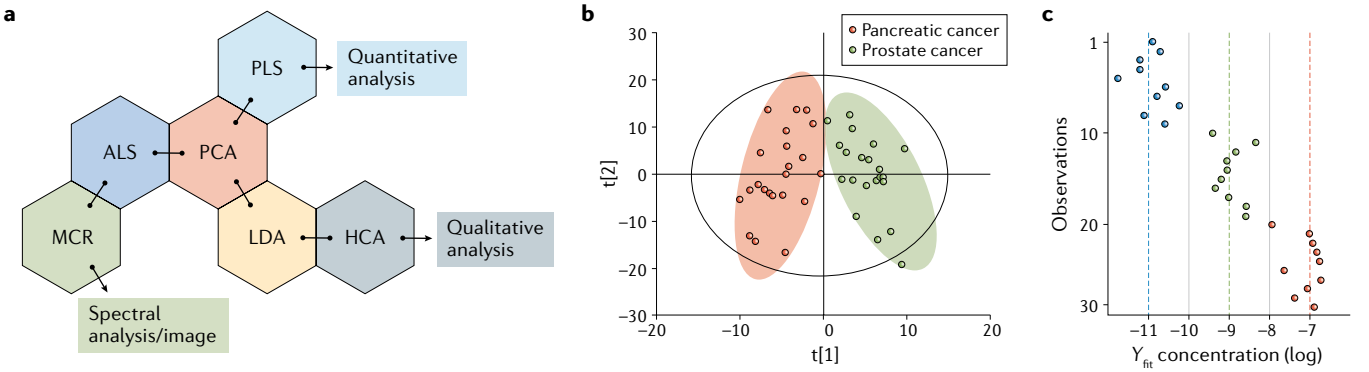

Fig. 5 | **Multivariate analysis of SERS data. a** | Chemometrics methods frequently used in surface-enhanced Raman spectroscopy (SERS). **b** | Orthogonal partial least squares (PLS) discriminant analysis for classification of pancreatic cancer (red) and prostate cancer (green). **c** | PLS regression concentration fitting of SERS spectra acquired from the groups of 10 pm (blue), 1 nm (green) and 100 nm (red). ALS, alternative least squares; HCA, hierarchical cluster analysis; LDA, linear discriminant analysis; MCR, multivariate curve resolution; PCA, principal component analysis. Part **b** adapted with permission from REF.[113], ACS. Part **c** adapted from REF.[115], CC BY 4.0 (https://creativecommons.org/licenses/by/4.0/).

Spectral analysis and SERS imaging. MCR combined with alternative least squares (MCR–ALS) is commonly used for analysis of Raman spectra and has recently been applied to SERS. MCR–ALS has been used with sample insertion constraint to deconvolute overlapping peaks in SERS spectra[116]. PCA has also been used on multiplexed molecular imaging of fresh tissues labelled with SERS-coded NPs[117], and MCR–ALS was used in the study of polymeric microfilms loaded with paracetamol[118].

SERS DFT theoretical calculation

DFT calculations are very useful to interpret SERS spectra[119,120]. For reproducing Raman spectra, harmonic approximation for prediction of vibrational frequencies using a scaling factor is sufficient; anharmonic approximation is not needed for general purposes[121–123].

Wu and colleagues[121,122,124] used DFT to study chemical enhancement of SERS spectroscopy in electronic interfaces. To investigate the structure of water adsorbed on silver, gold and platinum electrodes, DFT calculations were carried out for metal–water cluster models. The simulated Raman spectra of water–gold complexes[124] found that the relative intensity of the water–gold complex is very similar to that of water in the gas phase or a pure liquid. Adding a negative charge to the complex leads to significant enhancement of the Raman intensity.

Applications

SERS is an interdisciplinary technique that links physics, chemistry, nanotechnology, biology, biomedicine, food science, environmental science and forensic science. SERS-based methods are generally classified as intrinsic, combined or extrinsic SERS according to the origin of the obtained SERS fingerprints (TABLE 2).

The intrinsic SERS of adsorbates is useful for probing molecular structures, reactions or CT processes. Alternatively, ultrasensitive measurements are usually achieved by the extrinsic SERS of Raman reporters assembled with ligands of the target analytes. Another strategy that combines intrinsic and extrinsic SERS is useful for molecules with low affinity towards SERS-active materials. In this case, a reporter molecule is initially used to capture the target molecule via chemical reactions. In this way, the intrinsic SERS of both the capturing and target molecules are collected in one SERS spectrum. In this section, we review the latest applications of SERS specifically in chemistry, materials science and bioscience and highlight studies that exemplify key applications of SERS for surface reactions, interfacial CT for photovoltaic devices, biomolecular identification and intermolecular interactions, and chemical and biological sensing.

Surface reactions

Surface plasmons can redistribute excited electrons, inducing the CT enhancement of SERS mentioned above. The excited electrons can also transfer directly to the molecule and induce chemical reactions[125]. SERS has been applied in studies on plasmon-mediated chemical reactions (PMCRs), whereby molecules are directly attached to plasmonic metals. Plasmon-enhanced photocatalytic reactions can also be traced by SERS at a metal–semiconductor interface[126]. SERS is powerful for investigating electrocatalytic reactions in which the metal has a major role in Raman signal enhancement, and PMCRs are usually isolated by coating with oxides.

PMCRs represent a rapidly growing field of research[14], and photocatalytic reactions that occur in the absence of chemical reducing agents provide new opportunities for driving efficient light-to-energy conversion processes. Owing to the high correlation between plasmons and Raman scattering enhancement, SERS is useful for the in situ probing of PMCRs. As a typical example, a chemical transformation from PATP to 4,4′-dimercaptoazobenzene (DMAB) was unveiled via SERS on metals under an aerobic environment, where plasmon-induced enhanced electromagnetic fields, heat energy and hot electron–hole pairs all contributed to the molecular conversion[127]. Additionally, when PMCRs are isolated by coating the metal with oxides such as silicon dioxide, titanium dioxide or aluminium oxide, metal-oxide-catalysed or transition-metal-catalysed reactions can be revealed by SERS on plasmonic metals[128–130].

Potential-dependent SERS spectroscopy via electrochemical SERS (EC-SERS) is useful for revealing adsorption configurations and CT mechanisms[131]. In recent years, a growing number of electrocatalytic reactions, including oxygen reduction[132] and hydrogen oxidation[133], have been characterized by in situ EC-SERS[134]. EC-SERS allows for the sensitive identification of both the substrate and product, facilitating the in situ probing of vibrational information for catalytic processes. Plasmonic metals are generally used as SERS-active supports for catalytic transition metals and can also promote the electrocatalytic activity of semiconducting materials[135].

Interfacial charge transfer

Photovoltaics for the conversion of solar energy into electricity using semiconducting materials is a hot topic in materials science. Raman spectroscopy has been successfully applied for the direct dynamic investigation of charge separation in dye-sensitized solar cells (DSSCs)[136]. Hybridization of semiconductors with plasmonic metal nanomaterials is highly effective in improving CT efficiency, which allows for the rapid development of metal–semiconductor hybrid nanostructures in photovoltaic research[137]. Unprecedented SERS signals from metal–semiconductor heterostructures have been attributed to the synergistic contribution of plasmons and CT, allowing for the highly sensitive SERS-based probing of interfacial CT in photovoltaic devices[23]. Therefore, SERS-based studies on interfacial CT in metal–semiconductor heterostructures are beneficial for evaluating the CT efficiency of photovoltaic devices.

In metal–dye–semiconductor systems, similar to those in DSSCs (FIG. 6a), the SERS activity of the dye is dependent on the material type, size and morphology. Certain SERS marker bands of dyes (for example, N3: 1270 cm^{-1}; N719: 1266 cm^{-1})[138,139] are sensitive to CT at interfaces (FIG. 6c). With these band intensities, the contribution of CT to Raman signal enhancement can be estimated by the quantity ρ_{CT} (the degree of CT)[20]. CT efficiency at metal–semiconductor interfaces can thus be indirectly probed using ρ_{CT}, which is calculated from the SERS intensities of the dye molecules. Improved CT processes can be realized by modifying plasmonic metals or semiconductors to reduce the energy thresholds of dyes to materials (FIG. 6b). CT pathways at metal–semiconductor interfaces strongly depend on the nature of the metal or semiconductor, the probe molecule and their assembly method. At a metal–semiconductor interface, a CT transition from the metal to the semiconductor can occur through the mechanisms of plasmon-induced hot electron transfer (PHET) or plasmon-induced metal-to-semiconductor interfacial CT transition (PICTT). In these two cases, the hot electrons are either directly — through PICTT — or indirectly — with PHET — transferred to the adjacent semiconductor[23,140].

SERS is useful for probing the CT pathways in model structures for DSSCs. For such analyses, wavelength-dependent SERS is usually used to explore energy matching between the laser and the dyes. Hot electrons can be generated in dyes by excitation with the appropriate laser wavelength, followed by electron transfer to the conduction band of the semiconductor and further transfer to the metal[141]. This CT pathway is independent of surface plasmons, but plasmon-mediated pathways likely exist in such complicated systems. In recent years, increasing evidence for CT transitions in DSSC systems has been provided by SERS. SERS is helpful for optimizing the CT efficiency by modifying the metal, dye or semiconductor, which paves the way for the rational design of photovoltaic devices.

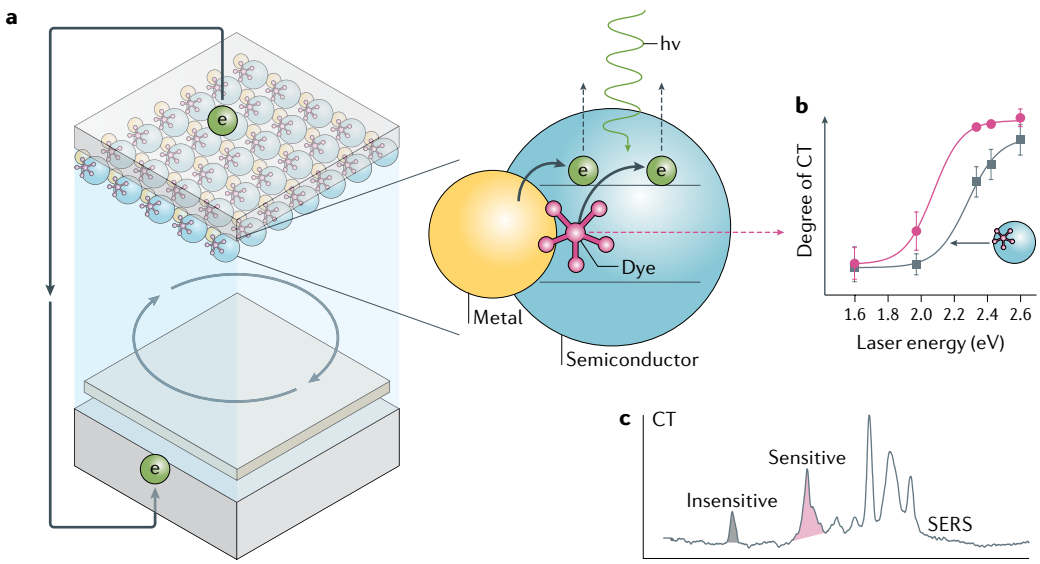

Fig. 6 | **Application of SERS to DSSCs. a** | Structure of a dye-sensitized solar cell (DSSC). Anode (top): the working electrode contains metals, dyes and semiconductors; cathode (bottom): the counter electrode. **b** | Degree of charge transfer (CT) at TiO_2–N3 (pink) and Ag–TiO_2–N3 (grey) interfaces. **c** | CT-sensitive (pink) and CT-insensitive (grey) bands in an N3 dye molecule. The two bands are specific for the N3 dye and are helpful for the ρ_{CT} calculation. SERS, surface-enhanced Raman spectroscopy. Parts **b** and **c** reprinted with permission from REF.[138], ACS.

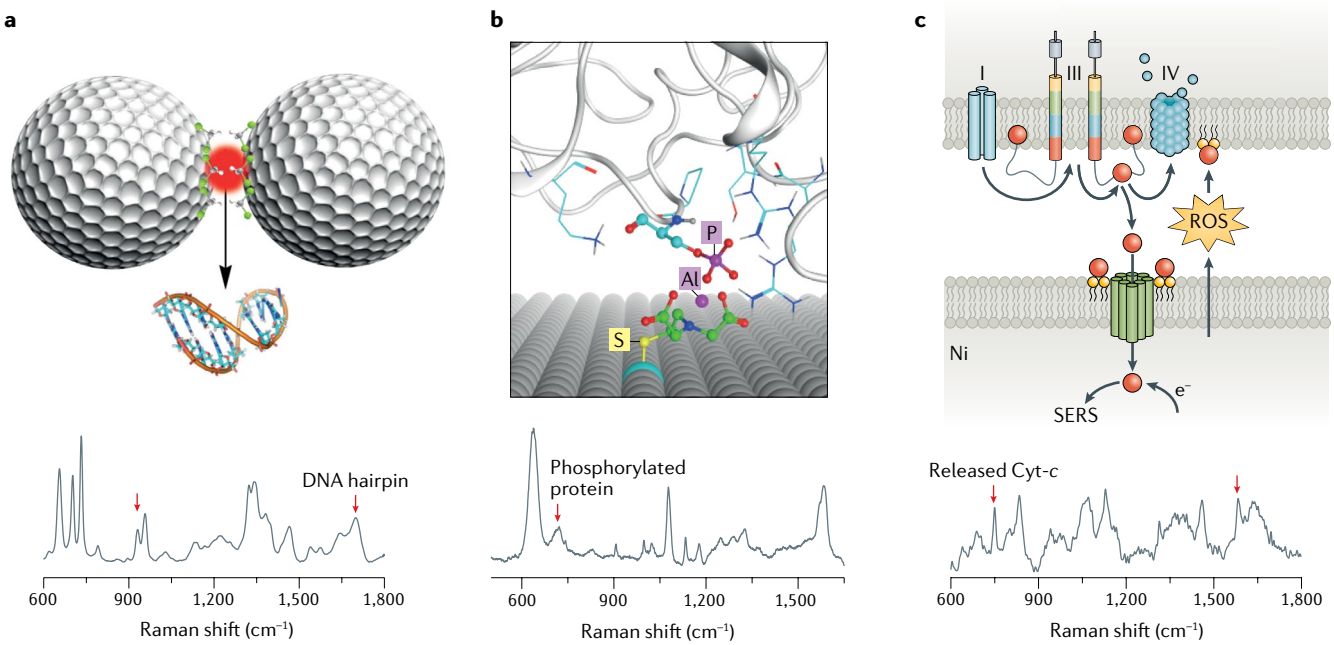

Fig. 7 | **Intrinsic SERS for the investigation of biomolecule structures. a** | DNA hairpin. **b** | Site-specific phosphorylated protein. **c** | Released cytochrome *c* (Cyt-*c*) from mitochondria. The characteristic surface-enhanced Raman spectroscopy (SERS) bands are marked with red arrows. ROS, reactive oxygen species. Part **a** adapted with permission from REF.[145], ACS. Part **b** adapted with permission from REF.[153], Elsevier. Part **c** adapted with permission from REF.[155], Wiley.

Intermolecular interactions

Numerous biomolecules, including proteins, DNA, RNA, lipids and carbohydrates, can be detected by intrinsic SERS. Proteins with cofactors, such as haem and flavin, are easily detected owing to the resonance effect with appropriate laser excitation. For biomolecules with low Raman cross-sections, such as peptides, nucleic acid bases and phospholipids, significant efforts have been made to improve their SERS activity by developing more sensitive SERS-active materials. The structural investigation of biomolecule–ligand interactions is crucial for the functional exploration of biological systems. However, direct contact between biomacromolecules and bare metals usually causes denaturation and poor SERS reproducibility; thus, biocompatible coatings and functionalization for metals are important for the SERS-based analysis of biological intermolecular interactions.

One useful approach to improving the SERS intensity of label-free DNAs is to aggregate the target molecules with silver NPs in an aqueous solution. The high affinity of iodide ions towards silver endows the former with a sort of cleaning function for silver surface NPs, which allows for highly reproducible SERS signals of DNA induced by aggregated reagents (such as magnesium and aluminium ions)[142]. The SERS band of the phosphate backbone is also helpful as an internal standard for quantifying nucleic acids with single-base sensitivity. This strategy offers a new way to detect single-stranded and double-stranded DNA for investigating DNA secondary structures such as i-motif, G-quadruplex and hairpin[143–145] (FIG. 7a) and identifying single-base mutations. Notably, the high spatial resolution of solid-state nanopores has enabled single-molecule DNA analysis based on SERS[146].

EC-SERS is powerful for the in situ probing of redox protein structures and reaction dynamics[147]. SERRS is sensitive to structural changes in redox centres such as haem, with Soret or Q-band excitation providing vibrational details regarding redox states, iron ligands and spin states. To improve the biocompatibility of silver surfaces, silver electrodes are usually coated with self-assembled monolayers of alkanethiolates to increase biocompatibility. Alternatively, nanostructured semiconductor electrodes can be used for direct protein immobilization[148]. Metal electrodes coated with self-assembled monolayers are most commonly used in this field owing to their unparalleled superiority in terms of SERS enhancement and conductivity. Based on EC-SERS, the role of cytochrome b_5 (Cyt-b_5) as an electron transfer shuttle and stabilizing electron source in enzymatic catalysis has been revealed[149], and slow and fast forms of cytochrome *c* (Cyt-*c*) oxidase have recently been characterized[150].

For proteins without cofactors, the major SERS bands of peptides originate from aromatic amino acid residues (phenylalanine, tyrosine and tryptophan) and histidine with an imidazole group. The intrinsic SERS of such proteins is rather weak on the typically employed metal NPs. Highly aggregated silver NPs in an acidic solution were found to be able to improve the SERS intensity and spectral reproducibility[151]. Note that the iodine-modified silver NPs mentioned above were also recently applied for the intrinsic SERS of native proteins[152]. On solid and bare SERS-active metals, a crosslinker of an appropriate length is effective at capturing label-free proteins while preserving the protein activity. This method is highly ultrasensitive to discriminate a single-site phosphorylated serine-396 in an intact Tau410 protein[153] (FIG. 7b).

Raman cross-sections
Dimensionally represents an effective area that is proportional to the Raman scattering rate at which a radiation–target interaction occurs.

Although it is still changing, SERS is feasible for analysing biomolecule intermolecular interactions. Nickel is more biocompatible than noble metals and has been developed as a SERS-active support for redox proteins. Interestingly, nickel is capable of transferring electrons to Cyt-b_5 and Cyt-*c*, enabling investigation of the electron transfer process from Cyt-b_5 to myoglobin[154]. Furthermore, nanostructured nickel supports have been applied to probe the interactions between the reduced form of Cyt-*c* and cardiolipin liposomes and even to trace the release process of Cyt-*c* from apoptotic mitochondria[155] (FIG. 7c). A first attempt to study cofactor-less protein–drug interactions by controlled protein immobilization was also recently reported[105]. Further experimental optimization for proteins with high molecular weights should be conducted, but this method offers a new possibility for SERS-based and label-free analyses of protein–ligand interactions at metal–liquid interfaces.

Chemical and biological sensing

The strategy of combined SERS facilitates the indirect detection of certain types of molecule according to the SERS of the product of a chemical reaction between a reporter molecule and the target molecule[156]. The concept allows for the detection of molecules with relatively low Raman cross-sections (such as oestrogens and phenols) by changing them to high Raman cross-section molecules before the SERS measurement. An efficient approach in this case has been demonstrated by functionalizing SERS-active NPs with a reporter molecule (such as PATP) that can capture anilines, phenols and their derivatives by an azo-coupling reaction[126]. Although the obtained spectra did not reflect the intrinsic SERS of the target molecules, the SERS fingerprints were still strongly dependent on the target molecule, indicating the multiplexing capability of such an approach. The highly sensitive SERRS signals of the azo products were attributed to the resonance effect, SERS effect and enrichment effect from the manganic cores. This method has potential applications in food safety and in controlling environmental pollutants. Alternatively, toxic chemicals on food surfaces can be easily detected by intrinsic SERS with flexible SERS substrates[157].

The SERS-based chemical sensing of inorganic ions (for example, mercury, lead, nitrogen dioxide and chromate) has been extensively studied owing to its important implications for the environment and biomedicine[103]. These ions are usually indirectly detected with Raman reporters by alteration of their SERS signal upon ion binding. The interaction of an inorganic ion with a reporter molecule may cause a significant change in the orientation of the reporter on the SERS-active surface or transform its chemical structure, resulting in frequency shifts or changes in relative intensities. Combining an aptamer with a Raman reporter has been demonstrated to be an efficient method for the highly sensitive detection of inorganic ions[158], in which the target ions recognize certain domains of the aptamer and thereby alter the original SERS intensity of the reporter.

SERS has widespread applications in biological sensing, including in vitro and in vivo biomarker detection, single-cell analysis and subcellular organelle targeting. As bio-samples usually involve complicated constituents, the label-free analysis of clinical samples such as serum and cells remains challenging owing to SERS spectral overlap. Thus, most SERS-based biological sensors are dependent on Raman reporters. The SERS intensity and frequency shifts of Raman reporters are both useful for biomarker detection. These reporters are commonly assembled with specific biomarker ligands, such as antibodies and aptamers, together with SERS-active NPs to yield what are known as SERS nanotags[159].

As a typical example, single-chain variable fragment (ScFv) antibodies — which are tumour-targeting ligands — that were conjugated with gold NPs were found to be capable of targeting epidermal growth factor receptors, an important tumour biomarker[160]. On the basis of biomarker–ligand recognition, biomarkers can be selectively quantified based on SERS of the reporters[161]. Notably, an antibody-free method for discriminating protein biomarkers in human serum was recently achieved according to the SERS relative intensity changes and frequency shifts of the reporter molecule, perylenetetracarboxylic acid[162].

When fabricated with various Raman reporters, SERS nanotags have multiplexing capabilities and have been applied in screening cancer cells, where they recognize membrane acceptors outside the cells[163]. SERS nanotags have also been introduced into cells for pH sensing at various cellular locations through a pH-sensitive molecule (such as 4-mercaptopyridine), or for label-free probing of drug metabolites[164,165]. With a biocompatible coating (such as polyethylene glycol and silica), SERS nanotags have been injected into a mouse model for tumour targeting[159]. SERS imaging is a straightforward method in which the typical signals of a Raman reporter in vivo can be quickly collected and subsequently integrated into an image. SERS nanotags enable highly sensitive tumour targeting and are helpful for in situ surgery guidance[159].

Reproducibility and data deposition

Reproducibility in SERS spectra relates to overall band intensities, relative intensities, frequency shifts and overall band frequencies. Here, we discuss the aspects of the SERS workflow that can affect each of these reproducibility factors.

SERS-active materials

The reproducibility of overall intensity of a SERS spectrum is highly dependent on the homogeneity and uniformity of the SERS-active materials. With the rapid development of SERS-active materials in recent years, nano-patterned and highly uniform substrates have become commercially available for practical applications, which has significantly improved the reproducibility of overall SERS intensity. Besides the overall intensity, SERS profiles may also suffer from fluctuations in relative intensity and frequency shifts owing to the interaction of the analytes with the SERS-active materials and the intermolecular interactions between the analytes. Random immobilization of a molecule via multiple binding groups will cause poor spectral reproducibility, and the analytes at different concentrations

might lead to different molecular orientations on the material surfaces[166].

Laser exposure time

The laser exposure time also affects SERS reproducibility by affecting spectral intensity and identification of the sample. Measurements with longer laser exposure times yield improved SNRs, but they may also cause the changes in spectral intensity and fingerprint owing to photobleaching. The photobleaching profiles of SERS nanotags originate from local photo-heating effects and photochemical reactions such as photo-oxidation and photoreduction. For intrinsic SERS, rotating the sample during measurement can help eliminate the photoreduction of redox proteins[167].

In the case of extrinsic SERS, methods for improving the photostability of SERS nanotags are crucial for measurements that require long exposure times, such as SERS imaging. An efficient approach for improving both the SERS intensity and photostability is to fabricate Raman reporters between particle gaps[168]. With a silica coating, these gap-enhanced Raman tags exhibited ultra-photostability, which significantly minimized spectral fluctuations during SERS image collection[168].

Frequency shifts

Quantifying analytes by frequency shifts has shown relatively higher degrees of reproducibility than that based on band intensities, which suffer from unavoidable intensity variation due to the inhomogeneity of SERS substrates. In a SERS-based immunoassay, key factors such as the solvent, antigens and antibodies have been shown to affect the frequency shifts of the Raman reporter[169]. Moreover, the random immobilization of biomacromolecules on a solid SERS substrate usually causes poor spectral reproducibility owing to the different orientations of multiple domains of the adsorbed molecules. This limitation can be overcome by functionalizing the material surface with a small crosslinker that can capture one site of the target molecule and thus control its homogeneous orientation[105].

Data storage

SERS data can be stored in different formats depending on spectrometer vendors' proprietary software. Data stored in ASCII or Microsoft Excel.csv format can be imported into Origin for graphing. Although there are Raman spectra databases that are free of charge or commercially available, there is currently no SERS data library accessible for SERS data sharing or reuse.

Limitations and optimizations

SERS has remarkable advantages over other spectroscopic methods, especially in terms of sensitivity and multiplexing ability. The major limitations related to mechanistic complexity, quantification accuracy and cytotoxicity are discussed below.

Mechanistic complexity

SERS enhancement mechanisms have been a controversial topic for decades[170]. In recent years, researchers have gained a deeper understanding of the importance of plasmons and the contribution of CT — as well as their synergistic effects — to SERS[3]. A clear understanding of these different mechanisms remains challenging owing to complexity from multiple contributions. The effects of other factors such as electromagnetic fields and heating energy on SERS have yet to be revealed[125].

Quantification accuracy

Numerous efforts have been made to improve SERS spectral intensities, but it remains a significant challenge to obtain a reproducible calibration curve or track batch-to-batch deviation across different labs based on the same quantitative method[171]. This is the reason why SERS has not been applied as a standard method for practical quantification analyses. Improving the accuracy will be a key issue that should be considered before designing and establishing a SERS-based analytical method[4]. Matrix effect is a major challenge for SERS-based detection and quantification in applications related to food science, environmental science and biomedicine[172]. Combining SERS with some separation methods such as Western blotting[173], high-performance liquid chromatography (HPLC)[174] and thin layer chromatography (TLC)[175] is helpful to separate target molecules and eliminate matrix effect. The combination of SERS with microfluidics enables rapid and repeatable analysis of multicomponent samples based on a continuous flow condition[176]. Alternatively, functionalizing substrates with specific antibodies and/or aptamers can selectively capture targets in matrices, with other species being removed with washing[177].

Cytotoxicity

Coating SERS-active materials with biocompatible materials is beneficial for SERS nanotags in cells to avoid any negative reactions of metals with cellular components such as cytoplasm and organelles[178]. NP-induced cytotoxicity is complicated and strongly dependent on NP properties such as surface coating, size, morphology and concentration, all of which affect SERS activity as well. Mitigating the cytotoxicity of one of these NP properties may negatively affect SERS activity[159]. Therefore, balancing the SERS activity and cytotoxicity is crucial for the SERS-based exploration of cells.

Understanding SERS mechanisms is of vital importance for guiding SERS applications. Theoretical methods such as DFT and time-dependent DFT calculations are helpful for revealing SERS mechanisms[179], although they have not been extensively applied in this area. Further efforts could be devoted to the rational design of SERS substrates with highly controlled size and morphology, combined with theoretical simulations, and such efforts will stimulate the further development of SERS mechanisms. In the past 10 years, the accuracy of SERS-based methods has gained increasing attention, and SERS spectral reproducibility has significantly improved, especially with the use of highly uniform SERS substrates[180]. Further efforts to optimize uniform SERS-active materials for accurate quantification should focus on their chemical stability and universality for the adsorption of various analytes.

Matrix effect
Complex matrices usually interfere with the surface-enhanced Raman spectroscopy signals of target molecules, reducing sensitivity and accuracy.

Prolonged exposure to SERS-active materials inevitably causes cytotoxicity[168]. Comprehensive investigation of factors that affect cytotoxicity, including SERS-active material type, concentration, morphology-dependent effects, toxic mechanisms, side effects and substrate removal mechanisms could be useful for SERS at the cellular or tissue level. Strategies for shortening the exposure time of the substrates could also be explored to minimize cytotoxicity, for example, by developing rapid scanning equipment for Raman imaging or fabricating magnetic SERS NPs to allow for rapid removal of NPs by an external magnetic field at a target location.

Outlook

Over the nearly five decades of its development, SERS has experienced significant growth in both fundamental and applied studies. Novel methods that can improve the current limitations are desirable, and the further development of SERS will be promising.

SERS-active organic semiconductors

The observation of SERS from nanostructured organic semiconducting films such as α,ω-diperfluorohexylquarterthiophene (DFH-4T)[181] extended the category of SERS-active nanostructures from inorganic materials to pure organic molecules. Such π-conjugated organic films exhibit excellent structural versatility, highly controllable morphology and tunable optoelectronic activities[182]. Attempts to study the SERS activity of other organic molecules, such as biological materials, are promising for solving the issue of biocompatibility with SERS substrates at the cellular or tissue level.

SERS and computational chemistry

Computational chemistry methods such as DFT, machine learning and molecular dynamics have important roles in SERS theoretical and applied science. Machine learning is an effective tool for predicting SERS signals[183], and integrating machine learning with SERS is a promising way to achieve high predictive accuracy even in complex matrices[184] and accelerate SERS applications in practical sensing devices. Data fusion strategies have great potential for improving the accuracy for species identification via integrating SERS and other spectroscopic data types[185]. Molecular dynamics simulations can provide information about the possibility of target molecule adsorption on nanomaterial surfaces, their orientation and their binding energies. Combining SERS with molecular dynamics[186] is effective for the rational design of biosensors and can reveal related enhancement mechanisms. Further exploration of SERS combined with computational chemistry will significantly improve the reliability and multiplexing ability of SERS-based methods.

High-spatial-resolution SERS imaging

The spatial resolution of Raman imaging can be significantly improved by combining Raman spectroscopy with atomic force microscopy, scanning near-field optical microscopy or scanning electron microscopy on solid materials[187]. By optimizing the experimental set-up, high-speed SERS imaging of individual NPs was achieved with a spatial resolution of ~7 nm (REF.[188]). However, SERS imaging with a high spatial resolution is still challenging in living cells. Near-infrared SERS imaging is helpful for tracking a single vesicle in a living cell, providing a way to monitor intracellular dynamics[189]. Currently, most organelles — with the exception of nuclei — cannot be recognized by typical SERS imaging of living cells. Label-free, non-invasive SERS cell imaging with a higher spatial resolution for analyses on the level of small organelles could be used to reveal signalling transduction in organelle cross-talk.

Combining SERS with SEIRAS

Raman and infrared spectroscopy are two complementary vibrational spectroscopies[2]. The combination of SERS and surface-enhanced infrared absorption spectroscopy (SEIRAS) allows for more detailed structural investigations of analytes with a high sensitivity[190]. SERS and SEIRAS have similar plasmon enhancement mechanisms, and 3D supercrystals of gold NPs were recently found to exhibit remarkable SERS and SEIRAS activities[191]. These supercrystals support multiple polaritonic resonances from the mid-infrared to near-infrared spectral range. Combining SERS with SEIRAS will be especially beneficial for the investigation of molecules with complicated structures, such as multi-enzyme complexes, to provide a structural basis and elucidate their reaction dynamics.

In summary, we have comprehensively reviewed SERS from its basic theories to its experimentation, results and applications. SERS reproducibility and limitations have been highlighted, and possible optimizations for more efficient design of the SERS systems are provided. Finally, promising directions for the field are proposed with the latest advances and challenges. Although difficulties remain, we believe SERS will be an increasingly powerful technique with the combined merits of ultra-sensitivity, high accuracy and excellent biocompatibility for practical applications.

Published online: 06 January 2022

1. Keresztury, G. in *Handbook of Vibrational Spectroscopy Raman Spectroscopy: Theory* (eds Chalmers, J. M. & Griffiths, P.) (Wiley, 2006).
2. Siebert, F. & Hildebrandt, P. *Theory of Infrared Absorption and Raman Spectroscopy* (Wiley, 2007).
3. Kneipp, K., Ozaki, Y. & Tian, Z.-Q. *Recent Developments in Plasmon-Supported Raman Spectroscopy (45 Years of Enhanced Raman Signals)* (World Scientific, 2017).
4. Zong, C. et al. Surface-enhanced raman spectroscopy for bioanalysis: reliability and challenges. *Chem. Rev.* **118**, 4946–4980 (2018).
5. Li, J.-F., Anema, J. R., Wandlowski, T. & Tian, Z.-Q. Dielectric shell isolated and graphene shell isolated nanoparticle enhanced Raman spectroscopies and their applications. *Chem. Soc. Rev.* **44**, 8399–8409 (2015).
6. Alessandri, I. & Lombardi, J. R. Enhanced Raman scattering with dielectrics. *Chem. Rev.* **116**, 14921–14981 (2016).
7. Fleischmann, M., Hendra, P. J. & McQuillan, A. J. Raman spectra of pyridine adsorbed at a silver electrode. *Chem. Phys. Lett.* **26**, 163–166 (1974). **This article is the first demonstration of the observation of SERS.**
8. Jeanmaire, D. L. R. & Duyne, R. P. V. Surface Raman spectroelectrochemistry: part I. Heterocyclic, aromatic, and aliphatic amines adsorbed on the anodized silver electrode. *J. Electroanal. Chem.* **84**, 1–20 (1977). **This article is one of two demonstrating the discovery of SERS.**
9. Albrecht, M. G. & Creighton, J. A. Anomalously intense Raman spectra of pyridine at a silver electrode. *J. Am. Chem. Soc.* **99**, 5215–5217 (1977). **This article is one of two demonstrating the discovery of SERS.**

10. Ding, S.-Y. et al. Nanostructure-based plasmon-enhanced Raman spectroscopy for surface analysis of materials. *Nat. Rev. Mater.* **1**, 16021 (2016).
11. Itoh, T., Yoshida, K. I., Tamaru, H., Biju, V. & Ishikawa, M. Experimental demonstration of the electromagnetic mechanism underlying surface enhanced Raman scattering using single nanoparticle spectroscopy. *J. Photoch. Photobio. Chem. A* **219**, 167–179 (2011).
12. Moskovits, M. Surface roughness and the enhanced intensity of Raman scattering by molecules adsorbed on metals. *J. Chem. Phys.* **69**, 4159–4161 (1978). **This article is the first demonstration of the role of surface plasmons in SERS**.
13. Willets, K. A. & Van Duyne, R. P. Localized surface plasmon resonance spectroscopy and sensing. *Annu. Rev. Phys. Chem.* **58**, 267–297 (2007).
14. Zhan, C. et al. From plasmon-enhanced molecular spectroscopy to plasmon-mediated chemical reactions. *Nat. Rev. Chem.* **2**, 216–230 (2018).
15. Hutter, E. & Fendler, J. H. Exploitation of localized surface plasmon resonance. *Adv. Mater.* **16**, 1685–1706 (2004).
16. Verma, P. Tip-enhanced Raman spectroscopy: technique and recent advances. *Chem. Rev.* **117**, 6447–6466 (2017).
17. Han, X. X., Ji, W., Zhao, B. & Ozaki, Y. Semiconductor-enhanced Raman scattering: active nanomaterials and applications. *Nanoscale* **9**, 4847–4861 (2017).
18. Chowdhury, J. How the charge transfer (CT) contributions influence the SERS spectra of molecules? A retrospective from the view of albrecht's "A" and Herzberg–Teller contributions. *Appl. Spectrosc. Rev.* **50**, 240–260 (2015).
19. Gersten, J. I., Birke, R. L. & Lombardi, J. R. Theory of enhance l light scattering from molecules adsorbed at the metal-solution interface. *Phys. Rev. Lett.* **43**, 147–150 (1979). **This article is the first demonstration of CT contribution to SERS**.
20. Lombardi, J. R. & Birke, R. L. A unified view of surface-enhanced raman scattering. *Acc. Chem. Res.* **42**, 734–742 (2009).
21. Lombardi, J. R. & Birke, R. L. The theory of surface-enhanced Raman scattering. *J. Chem. Phys.* **136**, 144704 (2012).
22. Lombardi, J. R. & Birke, R. L. Theory of surface-enhanced raman scattering in semiconductors. *J. Phys. Chem. C.* **118**, 11120–11130 (2014).
23. Liu, Y., Ma, H., Han, X. X. & Zhao, B. Metal–semiconductor heterostructures for surface-enhanced Raman scattering: synergistic contribution of plasmons and charge transfer. *Mater. Horiz.* **8**, 370–382 (2021).
24. Sharma, B., Frontiera, R. R., Henry, A.-I., Ringe, E. & Van Duyne, R. P. SERS: materials, applications, and the future. *Mater. Today* **15**, 16–25 (2012).
25. Pérez-Jiménez, A. I., Lyu, D., Lu, Z., Liu, G. & Ren, B. Surface-enhanced Raman spectroscopy: benefits, trade-offs and future developments. *Chem. Sci.* **11**, 4563–4577 (2020).
26. Willets, K. A. Super-resolution imaging of SERS hot spots. *Chem. Soc. Rev.* **43**, 3854–3864 (2014).
27. Yang, Z., Li, Q., Fang, Y. & Sun, M. Deep ultraviolet tip-enhanced Raman scattering. *Chem. Commun.* **47**, 9131–9133 (2011).
28. Palonpon, A. F. et al. Raman and SERS microscopy for molecular imaging of live cells. *Nat. Protoc.* **8**, 677–692 (2013).
29. Schlücker, S., Schaeberle, M. D., Huffman, S. W. & Levin, I. W. Raman microspectroscopy: a comparison of point, line, and wide-field imaging methodologies. *Anal. Chem.* **75**, 4312–4318 (2003).
30. Smith, R., Wright, K. L. & Ashton, L. Raman spectroscopy: an evolving technique for live cell studies. *Analyst* **141**, 3590–3600 (2016).
31. Stöckle, R. M., Suh, Y. D., Deckert, V. & Zenobi, R. Nanoscale chemical analysis by tip-enhanced Raman spectroscopy. *Chem. Phys. Lett.* **318**, 131–136 (2000). **This article presents the first conceptual demonstration of TERS**.
32. Anderson, M. S. Locally enhanced Raman spectroscopy with an atomic force microscope. *App. Phys. Lett.* **76**, 3130–3132 (2000).
33. Zhang, Z., Sheng, S., Wang, R. & Sun, M. Tip-enhanced raman spectroscopy. *Anal. Chem.* **88**, 9328–9346 (2016).
34. Hayazawa, N., Inouye, Y., Sekkat, Z. & Kawata, S. Metallized tip amplification of near-field Raman scattering. *Opt. Comm.* **183**, 333–336 (2000).
35. Yeo, B.-S., Stadler, J., Schmid, T., Zenobi, R. & Zhang, W. Tip-enhanced Raman spectroscopy–its status, challenges and future directions. *Chem. Phys. Lett.* **472**, 1–13 (2009).
36. Jiang, N. et al. Observation of multiple vibrational modes in ultrahigh vacuum tip-enhanced Raman spectroscopy combined with molecular-resolution scanning tunneling microscopy. *Nano Lett.* **12**, 5061–5067 (2012).
37. Kurouski, D., Zaleski, S., Casadio, F., Van Duyne, R. P. & Shah, N. C. Tip-enhanced raman spectroscopy (TERS) for in situ identification of indigo and iron gall ink on paper. *J. Am. Chem. Soc.* **136**, 8677–8684 (2014).
38. Tian, Z. Q., Ren, B. & Mao, B. W. Extending surface raman spectroscopy to transition metal surfaces for practical applications. 1. Vibrational properties of thiocyanate and carbon monoxide adsorbed on electrochemically activated platinum surfaces. *J. Phys. Chem. B* **101**, 1338–1346 (1997). **This article is the first demonstration of SERS on a transition metal**.
39. Pilot, R. et al. A review on surface-enhanced Raman scattering. *Biosensors* **9**, 57 (2019).
40. Yamada, H., Yamamoto, Y. & Tani, N. Surface-enhanced Raman scattering (SERS) of adsorbed molecules on smooth surfaces of metals and a metal oxide. *Chem. Phys. Lett.* **86**, 397–400 (1982). **This article is the first demonstration of SERS on a semiconducting material**.
41. Lin, X.-M., Cui, Y., Xu, Y.-H., Ren, B. & Tian, Z.-Q. Surface-enhanced Raman spectroscopy: substrate-related issues. *Anal. Bioanal. Chem.* **394**, 1729–1745 (2009).
42. Halas, N. J. & Moskovits, M. Surface-enhanced Raman spectroscopy: substrates and materials for research and applications. *MRS Bull.* **38**, 607–611 (2013).
43. Slepička, P., Slepičková Kasálková, N., Siegel, J., Kolská, Z. & Švorčík, V. Methods of gold and silver nanoparticles preparation. *Materials* **13**, 1 (2019).
44. Frens, G. Controlled nucleation for the regulation of the particle size in monodisperse gold suspensions. *Nat. Phys. Sci.* **241**, 20–22 (1973).
45. Lee, P. C. & Meisel, D. Adsorption and surface-enhanced Raman of dyes on silver and gold sols. *J. Phys. Chem. C.* **86**, 3391–3395 (1982).
46. Kang, H. et al. Stabilization of silver and gold nanoparticles: preservation and improvement of plasmonic functionalities. *Chem. Rev.* **119**, 664–699 (2019).
47. Guerrini, L., Alvarez-Puebla, R. A. & Pazos-Perez, N. Surface modifications of nanoparticles for stability in biological fluids. *Materials* **11**, 1154 (2018).
48. Liebig, F. et al. Spiked gold nanotriangles: formation, characterization and applications in surface-enhanced Raman spectroscopy and plasmon-enhanced catalysis. *RSC Adv.* **10**, 8152–8160 (2020).
49. Garcia-Leis, A., Garcia-Ramos, J. V. & Sanchez-Cortes, S. Silver nanostars with high SERS performance. *J. Phys. Chem. C.* **117**, 7791–7795 (2013).
50. Kundu, S. A new route for the formation of Au nanowires and application of shape-selective Au nanoparticles in SERS studies. *J. Mater. Chem. C.* **1**, 831–842 (2012).
51. Roy, S., Ajmal, C. M., Baik, S. & Kim, J. Silver nanoflowers for single-particle SERS with 10 pM sensitivity. *Nanotechnology* **28**, 465705 (2017).
52. Chang, H.-H. & Murphy, C. J. Mini gold nanorods with tunable plasmonic peaks beyond 1000 nm. *Chem. Mater.* **30**, 1427–1435 (2018).
53. Cohen-Pope, S. et al. Morphology control of SERS-active 2D gold nanosnowflakes. *J. Mater. Chem. C.* **8**, 12427–12436 (2020).
54. Rodriguez, R. D. et al. Aluminum and copper nanostructures for surface-enhanced Raman spectroscopy: a one-to-one comparison to silver and gold. *Sens. Actuators B Chem* **262**, 922–927 (2018).
55. Yang, B. et al. Recent development of SERS technology: semiconductor-based study. *ACS Omega* **4**, 20101–20108 (2019).
56. Xu, L., Liang, H.-W., Yang, Y. & Yu, S.-H. Stability and reactivity: positive and negative aspects for nanoparticle processing. *Chem. Rev.* **118**, 3209–3250 (2018).
57. Dick, L. A., McFarland, A. D., Haynes, C. L. & Van Duyne, R. P. Metal film over nanosphere (MFON) electrodes for surface-enhanced raman spectroscopy (SERS): improvements in surface nanostructure stability and suppression of irreversible loss. *J. Phys. Chem. B* **106**, 853–860 (2002).
58. Wang, J. F., Wu, X. Z., Xiao, R., Dong, P. T. & Wang, C. G. Performance-enhancing methods for au film over nanosphere surface-enhanced raman scattering substrate and melamine detection application. *PLoS ONE* **9**, e97976 (2014).
59. Styles, M. J. et al. Optimization of film over nanosphere substrate fabrication for SERS sensing of the allergen soybean agglutinin. *J. Raman. Spectrosc.* **52**, 482–490 (2021).
60. Liao, P. F. in *Surface Enhanced Raman Scattering* (eds Chang, R. K. & Furtak, T. E.) 379–390 (Springer, 1982).
61. Petti, L. et al. A plasmonic nanostructure fabricated by electron beam lithography as a sensitive and highly homogeneous SERS substrate for bio-sensing applications. *Vib. Spectrosc.* **82**, 22–30 (2016).
62. Dhawan, A. et al. Methodologies for developing surface-enhanced raman scattering (SERS) substrates for detection of chemical and biological molecules. *IEEE Sens. J.* **10**, 608–616 (2010).
63. Abu Hatab, N. A., Oran, J. M. & Sepaniak, M. J. Surface-enhanced Raman spectroscopy substrates created via electron beam lithography and nanotransfer printing. *ACS Nano* **2**, 377–385 (2008).
64. Haynes, C. L. & Van Duyne, R. P. Plasmon-sampled surface-enhanced raman excitation spectroscopy. *J. Phys. Chem. B* **107**, 7426–7433 (2003).
65. Guo, Y. et al. Molecular sensitivities of substrate-supported gold nanocrystals. *J. Phys. Chem. C* **123**, 7336–7346 (2019).
66. Szlag, V. M. et al. Molecular affinity agents for intrinsic surface-enhanced raman scattering (SERS) sensors. *ACS Appl. Mater. Interfaces* **10**, 31825–31844 (2018).
67. Rodriguez, R. S. et al. Sensing food contaminants: advances in analytical methods and techniques. *Anal. Chem.* **93**, 23–40 (2021).
68. Tripp, R. A., Dluhy, R. A. & Zhao, Y. Novel nanostructures for SERS biosensing. *Nano Today* **3**, 31–37 (2008).
69. Bantz, K. C. et al. Recent progress in SERS biosensing. *Phys. Chem. Chem. Phys.* **13**, 11551–11567 (2011).
70. Nie, S. & Emory, S. R. Probing single molecules and single nanoparticles by surface-enhanced Raman scattering. *Science* **275**, 1102–1106 (1997). **This article is one of two presenting the first conceptual demonstration of single-molecule SERS**.
71. Kneipp, K. et al. Single molecule detection using surface-enhanced raman scattering (SERS). *Phys. Rev. Lett.* **78**, 1667–1670 (1997). **This article is one of two presenting the first conceptual demonstration of single-molecule SERS**.
72. Scott, B. L. & Carron, K. T. Dynamic surface enhanced raman spectroscopy (SERS): extracting SERS from normal raman scattering. *Anal. Chem.* **84**, 8448–8451 (2012).
73. Scott, B. L. & Carron, K. T. Dynamic raman scattering studies of coated gold nanoparticles: 4-mercaptopyridine, 4-mercaptophenol, and benzenethiol. *J. Phys. Chem. C.* **120**, 20905–20913 (2016).
74. Zong, C. et al. Single-molecule level rare events revealed by dynamic surface-enhanced raman spectroscopy. *Anal. Chem.* **92**, 15806–15810 (2020).
75. Lindquist, N. C. & Brolo, A. G. Ultra-high-speed dynamics in surface-enhanced raman scattering. *J. Phys. Chem. C.* **125**, 7523–7532 (2021).
76. Song, J. E., Kim, H., Lee, S. W. & Cho, E. C. Nanoscale structural switching of plasmonic nanograin layers on hydrogel colloidal monolayers for highly sensitive and dynamic SERS in water with areal signal reproducibility. *Anal. Chem.* **89**, 11259–11268 (2017).
77. He, Y., Yang, X., Yuan, R. & Chai, Y. Switchable target-responsive 3D DNA hydrogels as a signal amplification strategy combining with SERS technique for ultrasensitive detection of miRNA 155. *Anal. Chem.* **89**, 8538–8544 (2017).
78. Zhang, C., Liu, X., Xu, Z. & Liu, D. Multichannel stimulus-responsive nanoprobes for H_2O_2 sensing in diverse biological milieus. *Anal. Chem.* **92**, 12639–12646 (2020).
79. Zheng, Y. et al. Reversible gating of smart plasmonic molecular traps using thermoresponsive polymers for single-molecule detection. *Nat. Commun.* **6**, 8797 (2015).
80. Jahn, I. J. et al. Surface-enhanced Raman spectroscopy and microfluidic platforms: challenges, solutions and potential applications. *Analyst* **142**, 1022–1047 (2017).
81. Jeon, J. et al. SERS-based droplet microfluidics for high-throughput gradient analysis. *Lab. Chip* **19**, 674–681 (2019).

82. Kim, D. et al. Microfluidic-SERS devices for one shot limit-of-detection. *Analyst* **139**, 3227–3234 (2014).
83. Bai, S., Serien, D., Hu, A. & Sugioka, K. 3D microfluidic surface-enhanced raman spectroscopy (SERS) chips fabricated by all-femtosecond-laser-processing for real-time sensing of toxic substances. *Adv. Funct. Mater.* **28**, 1706262 (2018).
84. Wang, Z., Ye, S., Zhang, N., Liu, X. & Wang, M. Triggerable mutually amplified signal probe based SERS-microfluidics platform for the efficient enrichment and quantitative detection of miRNA. *Anal. Chem.* **91**, 5043–5050 (2019).
85. Zhu, J. et al. Highly sensitive and label-free determination of thiram residue using surface-enhanced Raman spectroscopy (SERS) coupled with paper-based microfluidics. *Anal. Methods* **9**, 6186–6193 (2017).
86. Almehmadi, L. M., Curley, S. M., Tokranova, N. A., Tenenbaum, S. A. & Lednev, I. K. Surface enhanced Raman spectroscopy for single molecule protein detection. *Sci. Rep.* **9**, 12356 (2019).
87. Lussier, F. et al. Dynamic SERS nanosensor for neurotransmitter sensing near neurons. *Faraday Discuss.* **205**, 387–407 (2017).
88. Ofner, J. et al. Tip-enhanced Raman spectroscopy of atmospherically relevant aerosol nanoparticles. *Anal. Chem.* **88**, 9766–9772 (2016).
89. Park, K.-D. et al. Hybrid tip-enhanced nanospectroscopy and nanoimaging of monolayer WSe2 with local strain control. *Nano Lett.* **16**, 2621–2627 (2016).
90. Faucett, A. C. & Mativetsky, J. M. Nanoscale reduction of graphene oxide under ambient conditions. *Carbon* **95**, 1069–1075 (2015).
91. Picardi, G. et al. Exchange of methyl- and azobenzene-terminated alkanethiols on polycrystalline gold studied by tip-enhanced raman mapping. *ChemPhysChem* **15**, 276–282 (2014).
92. Xie, W. & Schlücker, S. Hot electron-induced reduction of small molecules on photorecycling metal surfaces. *Nat. Commun.* **6**, 7570 (2015).
93. Zhang, Z., Deckert-Gaudig, T. & Deckert, V. Label-free monitoring of plasmonic catalysis on the nanoscale. *Analyst* **140**, 4325–4335 (2015).
94. Lu, G. et al. Live-cell SERS endoscopy using plasmonic nanowire waveguides. *Adv. Mater.* **26**, 5124–5128 (2014).
95. Schlücker, S. et al. Immuno-Raman microspectroscopy: in situ detection of antigens in tissue specimens by surface-enhanced Raman scattering. *J. Raman. Spectrosc.* **37**, 719–721 (2006).
96. Lutz, B. R. et al. Spectral analysis of multiplex raman probe signatures. *ACS Nano* **2**, 2306–2314 (2008).
97. Du, Z., Qi, Y., He, J., Zhong, D. & Zhou, M. Recent advances in applications of nanoparticles in SERS in vivo imaging. *WIRES Nanomed. Nanobi.* **13**, e1672 (2021).
98. Olson, A. P., Spies, K. B., Browning, A. C., Soneral, P. A. G. & Lindquist, N. C. Chemically imaging bacteria with super-resolution SERS on ultra-thin silver substrates. *Sci. Rep.* **7**, 9135 (2017).
99. Stranahan, S. M. & Willets, K. A. Super-resolution optical imaging of single-molecule SERS hot spots. *Nano Lett.* **10**, 3777–3784 (2010).
100. Socrates, G. *Infrared and Raman Characteristic Group Frequencies: Tables and Charts* (John Wiley & Sons, 2004).
101. Procházka, M. *Surface-Enhanced Raman Spectroscopy* (Springer, 2016).
102. Bell, S. E. J. & Sirimuthu, N. M. S. Quantitative surface-enhanced Raman spectroscopy. *Chem. Soc. Rev.* **37**, 1012–1024 (2008).
103. Ji, W., Li, L., Zhang, Y., Wang, X. & Ozaki, Y. Recent advances in surface-enhanced Raman scattering-based sensors for the detection of inorganic ions: sensing mechanism and beyond. *J. Raman. Spectrosc.* **52**, 468–481 (2021).
104. Schlücker, S. *Surface Enhanced Raman Spectroscopy: Analytical, Biophysical and Life Science Applications* (Wiley, 2010).
105. Ma, H. et al. Surface-enhanced Raman scattering for direct protein function investigation: controlled immobilization and orientation. *Anal. Chem.* **91**, 8767–8771 (2019).
106. Mao, Z. et al. Multiphonon resonant Raman scattering and photoinduced charge-transfer effects at ZnO–molecule interfaces. *J. Phys. Chem. C.* **116**, 26908–26918 (2012).
107. Kitahama, Y., Egashira, M., Suzuki, T., Tanabe, I. & Ozaki, Y. Sensitive marker bands for the detection of spin states of heme in surface-enhanced resonance Raman scattering spectra of metmyoglobin. *Analyst* **139**, 6421–6425 (2014).
108. Kitagawa, T. & Ozaki, Y. in *Metal Complexes with Tetrapyrrole Ligands volume I* (ed. Buchler, J. W.) 71–114 (Springer, 1987).
109. Kang, B., Austin, L. A. & El-Sayed, M. A. Real-time molecular imaging throughout the entire cell cycle by targeted plasmonic-enhanced Rayleigh/Raman spectroscopy. *Nano Lett.* **12**, 5369–5375 (2012).
110. Vantasin, S. et al. 3D SERS imaging using chemically synthesized highly symmetric nanoporous silver microparticles. *Angew. Chem. Int. Ed.* **55**, 8391–8395 (2016).
111. Jarvis, R. M. & Goodacre, R. Discrimination of bacteria using surface-enhanced Raman spectroscopy. *Anal. Chem.* **76**, 40–47 (2004).
112. Lin, J. et al. Label-free optical detection of type II diabetes based on surface-enhanced Raman spectroscopy and multivariate analysis. *J. Raman. Spectrosc.* **45**, 884–889 (2014).
113. Phyo, J. B. et al. Label-free SERS Analysis of urine using a 3D-stacked AgNW-glass fiber filter sensor for the diagnosis of pancreatic cancer and prostate cancer. *Anal. Chem.* **93**, 3778–3785 (2021).
114. Zong, M. et al. Comparison of surface-enhanced Raman scattering properties of serum and urine for the detection of chronic kidney disease in patients. *Appl. Spectrosc.* **75**, 412–421 (2021).
115. Yasukuni, R. et al. Quantitative analysis of SERS spectra of MnSOD over fluctuated aptamer signals using multivariate statistics. *Nanophotonics* **8**, 1477–1483 (2019).
116. Sricharoen, N. et al. MCR-ALS with sample insertion constraint to enhance the sensitivity of surface-enhanced Raman scattering detection. *Analyst* **146**, 3251–3262 (2021).
117. Wang, Y., Kang, S., Doerksen, J. D., Glaser, A. K. & Liu, J. T. C. Surgical guidance via multiplexed molecular imaging of fresh tissues labeled with SERS-coded nanoparticles. *IEEE J. Quantum Electron.* **22**, 154–164 (2015).
118. Mamián-López, M. B. & Poppi, R. J. SERS hyperspectral imaging assisted by MCR-ALS for studying polymeric microfilms loaded with paracetamol. *Microchem. J.* **123**, 243–251 (2015).
119. Wójcik M. J., Nakatsuji, H., Kirtman, B. & Ozaki, Y. *Frontiers of Quantum Chemistry* (Springer, 2017).
120. Ozaki, Y., Wójcik, M. J., Popp, J. *Molecular Spectroscopy: A Quantum Chemistry Approach* (Wiley, 2019).
121. Pang, R., Wu, D.-Y. & Tian, Z.-Q. in *Frontiers of Quantum Chemistry* (eds Wójcik, M. J., Nakatsuji, H., Kirtman, B. & Ozaki, Y.) 455–482 (Springer, 2018).
122. Wu, D. Y., Chen, Y. L., Wu, Y. F. & Tian, Z. Q. in *Molecular Spectroscopy: A Quantum Chemistry Approach* Vol. 2 (eds Wójcik, M. J., Ozaki, Y. & Popp, J.) 537–573 (Wiley-VCH, 2019).
123. Mueller, C. M., Gieseking, L. M. & Schatz, G. C. *Molecular Spectroscopy: A Quantum Chemistry Approach* (John Wiley & Sons, 2019).
124. Li, J.-F. et al. SERS and DFT study of water on metal cathodes of silver, gold and platinum nanoparticles. *Phys. Chem. Chem. Phys.* **12**, 2493–2502 (2010).
125. Zhan, C., Chen, X.-J., Huang, Y.-F., Wu, D.-Y. & Tian, Z.-Q. Plasmon-mediated chemical reactions on nanostructures unveiled by surface-enhanced raman spectroscopy. *Acc. Chem. Res.* **52**, 2784–2792 (2019).
126. Han, X. X. et al. Magnetic titanium dioxide nanocomposites for surface-enhanced resonance Raman spectroscopic determination and degradation of toxic anilines and phenols. *Angew. Chem. Int. Ed.* **53**, 2481–2484 (2014).
127. Zhan, C. et al. Interfacial construction of plasmonic nanostructures for the utilization of the plasmon-excited electrons and holes. *J. Am. Chem. Soc.* **141**, 8053–8057 (2019).
128. Li, Y. et al. C–H arylation on nickel nanoparticles monitored by in situ surface-enhanced Raman spectroscopy. *Angew. Chem. Int. Ed.* **58**, 9049–9053 (2019).
129. Zhang, K. et al. Synthesis of a gold–metal oxide core–satellite nanostructure for in situ SERS study of CuO-catalyzed photooxidation. *Angew. Chem. Int. Ed.* **59**, 18003–18009 (2020).
130. Wei, J. et al. Probing single-atom catalysts and catalytic reaction processes by shell-isolated nanoparticle-enhanced Raman spectroscopy. *Angew. Chem. Int. Ed.* **60**, 9306–9310 (2021).
131. Wu, D.-Y., Li, J.-F., Ren, B. & Tian, Z.-Q. Electrochemical surface-enhanced Raman spectroscopy of nanostructures. *Chem. Soc. Rev.* **37**, 1025–1041 (2008).
132. Ze, H. J. et al. Molecular insight of the critical role of Ni in Pt-based nanocatalysts for improving the oxygen reduction reaction probed using an in situ SERS borrowing strategy. *J. Am. Chem. Soc.* **143**, 1318–1322 (2021).
133. Wang, Y.-H. et al. Spectroscopic verification of adsorbed hydroxy intermediates in the bifunctional mechanism of the hydrogen oxidation reaction. *Angew. Chem. Int. Ed.* **60**, 5708–5711 (2021).
134. Hess, C. New advances in using Raman spectroscopy for the characterization of catalysts and catalytic reactions. *Chem. Soc. Rev.* **50**, 3519–3564 (2021).
135. Du, L. et al. Plasmon-promoted electrocatalytic water splitting on metal–semiconductor nanocomposites: the interfacial charge transfer and the real catalytic sites. *Chem. Sci.* **10**, 9605–9612 (2019).
136. Mao, Z. et al. Direct dynamic evidence of charge separation in a dye-sensitized solar cell obtained under operando conditions by Raman spectroscopy. *Angew. Chem. Int. Ed.* **59**, 10780–10784 (2020).
137. Liu, X. et al. Noble metal–metal oxide nanohybrids with tailored nanostructures for efficient solar energy conversion, photocatalysis and environmental remediation. *Energy Environ. Sci.* **10**, 402–434 (2017).
138. Wang, X., Zhao, B., Li, P., Han, X. X. & Ozaki, Y. Charge transfer at the TiO_2/N3/Ag interface monitored by surface-enhanced Raman spectroscopy. *J. Phys. Chem. C* **121**, 5145–5153 (2017).
139. Wang, X. et al. Investigation of charge transfer in Ag/N719/TiO_2 interface by surface-enhanced raman spectroscopy. *J. Phys. Chem. C* **120**, 13078–13086 (2016).
140. Wu, K., Chen, J., McBride, J. R. & Lian, T. Efficient hot-electron transfer by a plasmon-induced interfacial charge-transfer transition. *Science* **349**, 632 (2015).
141. Wang, Y., Liu, J., Ozaki, Y., Xu, Z. & Zhao, B. Effect of TiO_2 on altering direction of interfacial charge transfer in a TiO_2-Ag-MPY-FePc system by SERS. *Angew. Chem. Int. Ed.* **58**, 8172–8176 (2019).
142. Xu, L.-J. et al. Label-free surface-enhanced Raman spectroscopy detection of DNA with single-base sensitivity. *J. Am. Chem. Soc.* **137**, 5149–5154 (2015).
143. Li, Y. et al. Structural features of DNA G-quadruplexes revealed by surface-enhanced raman spectroscopy. *J. Phys. Chem. Lett.* **9**, 3245–3252 (2018).
144. Li, Y. et al. Label-free detection of tetramolecular i-motifs by surface-enhanced Raman spectroscopy. *Anal. Chem.* **90**, 2996–3000 (2018).
145. Li, Y. et al. Direct approach toward label-free DNA detection by surface-enhanced Raman spectroscopy: discrimination of a single-base mutation in 50 base-paired double helixes. *Anal. Chem.* **91**, 7980–7984 (2019).
146. Chen, C. et al. High spatial resolution nanoslit SERS for single-molecule nucleobase sensing. *Nat. Commun.* **9**, 1733 (2018).
147. Murgida, D. H. & Hildebrandt, P. Disentangling interfacial redox processes of proteins by SERR spectroscopy. *Chem. Soc. Rev.* **37**, 937–945 (2008).
148. Öner, I. H. et al. High electromagnetic field enhancement of TiO_2 nanotube electrodes. *Angew.Chem. Int. Ed.* **57**, 7225–7229 (2018).
149. Kielb, P. et al. Spectroscopic observation of calcium-induced reorientation of cellobiose dehydrogenase immobilized on electrodes and its effect on electrocatalytic activity. *ChemPhysChem* **16**, 1960–1968 (2015).
150. Kruse, F. et al. A resonance Raman marker band characterizes the slow and fast form of cytochrome *c* oxidase. *J. Am. Chem. Soc.* **143**, 2769–2776 (2021).
151. Han, X. X., Huang, G. G., Zhao, B. & Ozaki, Y. Label-free highly sensitive detection of proteins in aqueous solutions using surface-enhanced Raman scattering. *Anal. Chem.* **81**, 3329–3333 (2009).
152. Bao, Y. et al. Label-free and highly sensitive detection of native proteins by Ag IANPs via surface-enhanced Raman spectroscopy. *Anal. Chem.* **92**, 14325–14329 (2020).
153. Ma, H. et al. In-situ fingerprinting phosphorylated proteins via surface-enhanced Raman spectroscopy: single-site discrimination of Tau biomarkers in Alzheimer's disease. *Biosens. Bioelectron.* **171**, 112748 (2021).
154. Han, X. X. et al. Nickel electrodes as a cheap and versatile platform for studying structure and function of immobilized redox proteins. *Anal. Chim. Acta* **941**, 35–40 (2016).
155. Zhu, J. et al. Redox-state-mediated regulation of cytochrome c release in apoptosis revealed by surface-enhanced Raman scattering on nickel substrates. *Angew. Chem. Int. Ed.* **58**, 16499–16503 (2019).

156. Han, X. X., Pienpinijtham, P., Zhao, B. & Ozaki, Y. Coupling reaction-based ultrasensitive detection of phenolic estrogens using surface-enhanced resonance Raman scattering. *Anal. Chem.* **83**, 8582–8588 (2011).
157. Li, Z., Huang, X. & Lu, G. Recent developments of flexible and transparent SERS substrates. *J. Mater. Chem. C* **8**, 3956–3969 (2020).
158. Fu, C. et al. DNAzyme-based plasmonic nanomachine for ultrasensitive selective surface-enhanced Raman scattering detection of lead ions via a particle-on-a-film hot spot construction. *Anal. Chem.* **86**, 11494–11497 (2014).
159. Lane, L. A., Qian, X. & Nie, S. SERS nanoparticles in medicine: from label-free detection to spectroscopic tagging. *Chem. Rev.* **115**, 10489–10529 (2015).
160. Qian, X. et al. In vivo tumor targeting and spectroscopic detection with surface-enhanced Raman nanoparticle tags. *Nat. Biotechnol.* **26**, 83–90 (2008).
161. Ma, H. et al. Multiplex immunochips for high-accuracy detection of AFP-L3% based on surface-enhanced Raman scattering: implications for early liver cancer diagnosis. *Anal. Chem.* **89**, 8877–8883 (2017).
162. Ma, H. et al. Antibody-free discrimination of protein biomarkers in human serum based on surface-enhanced Raman spectroscopy. *Analy. Chem.* **90**, 12342–12346 (2018).
163. Navas-Moreno, M. et al. Nanoparticles for live cell microscopy: a surface-enhanced Raman scattering perspective. *Sci. Rep.* **7**, 4471 (2017).
164. Shen, Y. et al. Organelle-targeting surface-enhanced Raman scattering (SERS) nanosensors for subcellular pH sensing. *Nanoscale* **10**, 1622–1630 (2018).
165. Han, G. et al. Label-free surface-enhanced Raman scattering imaging to monitor the metabolism of antitumor drug 6-mercaptopurine in living cells. *Anal. Chem.* **86**, 11503–11507 (2014).
166. Sun, C., Chen, T., Ruan, W., Zhao, B. & Cong, Q. Controlling the orientation of probe molecules on surface-enhanced Raman scattering substrates: A novel strategy to improve sensitivity. *Anal. Chim. Acta* **994**, 65–72 (2017).
167. Han, X. X. et al. Potential-dependent surface-enhanced resonance Raman spectroscopy at nanostructured TiO_2: a case study on cytochrome b_5. *Small* **9**, 4175–4181 (2013).
168. Zhang, Y., Gu, Y., He, J., Thackray, B. D. & Ye, J. Ultrabright gap-enhanced Raman tags for high-speed bioimaging. *Nat. Commun.* **10**, 3905 (2019).
169. Ma, H. et al. Frequency shifts in surface-enhanced Raman spectroscopy-based immunoassays: mechanistic insights and application in protein carbonylation detection. *Anal. Chem.* **91**, 9376–9381 (2019).
170. Kneipp, K., Moskovits, M. & Kneipp, H. *Surface-Enhanced Raman Scattering: Physics and Applications* (Springer, 2006).
171. Han, X. X., Ozaki, Y. & Zhao, B. Label-free detection in biological applications of surface-enhanced Raman scattering. *Trends Anal. Chem.* **38**, 67–78 (2012).
172. Filipec, S. V. et al. Influence of sample matrix on determination of histamine in fish by surface enhanced Raman spectroscopy coupled with chemometric modelling. *Foods* **10**, 1767 (2021).
173. Han, X. X. et al. Analytical technique for label-free multi-protein detection based on Western blot and surface-enhanced Raman scattering. *Anal. Chem.* **80**, 2799–2804 (2008).
174. Trachta, G., Schwarze, B., Sägmüller, B., Brehm, G. & Schneider, S. Combination of high-performance liquid chromatography and SERS detection applied to the analysis of drugs in human blood and urine. *J. Mol. Struct.* **693**, 175–185 (2004).
175. Takei, H. et al. TLC-SERS plates with a built-In SERS layer consisting of cap-shaped noble metal nanoparticles intended for environmental monitoring and food safety assurance. *J. Nanomater.* **2015**, 316189 (2015).
176. Pu, H., Xiao, W. & Sun, D.-W. SERS-microfluidic systems: a potential platform for rapid analysis of food contaminants. *Trends Food Sci. Technol.* **70**, 114–126 (2017).
177. Wang, H.-X., Zhao, Y.-W., Li, Z., Liu, B.-S. & Zhang, D. Development and application of aptamer-based surface-enhanced Raman spectroscopy sensors in quantitative analysis and biotherapy. *Sensors* **19**, 3806 (2019).
178. Zavaleta, C. L. et al. Multiplexed imaging of surface enhanced Raman scattering nanotags in living mice using noninvasive Raman spectroscopy. *Proc. Natl Acad. Sci. USA* **106**, 13511 (2009).
179. Ji, W., Kitahama, Y., Xue, X., Zhao, B. & Ozaki, Y. Generation of pronounced resonance profile of charge-transfer contributions to surface-enhanced Raman scattering. *J. Phys. Chem. C* **116**, 2515–2520 (2012).
180. Das, G. et al. Nano-patterned SERS substrate: application for protein analysis vs. temperature. *Biosens. Bioelectron.* **24**, 1693–1699 (2009).
181. Yilmaz, M. et al. Nanostructured organic semiconductor films for molecular detection with surface-enhanced Raman spectroscopy. *Nat. Mater.* **16**, 918–924 (2017).
This article is the first conceptual demonstration of SERS-active organic semiconductor films.
182. Demirel, G. et al. Molecular engineering of organic semiconductors enables noble metal-comparable SERS enhancement and sensitivity. *Nat. Commun.* **10**, 5502 (2019).
183. Hu, W. et al. Machine learning protocol for surface-enhanced Raman spectroscopy. *J. Phys. Chem. Lett.* **10**, 6026–6031 (2019).
184. Leong, Y. X. et al. Surface-enhanced Raman scattering (SERS) taster: a machine-learning-driven multireceptor platform for multiplex profiling of wine flavors. *Nano Lett.* **21**, 2642–2649 (2021).
185. Han, Z. Z. et al. SERS and MALDI-TOF MS based plasma exosome profiling for rapid detection of osteosarcoma. *Analyst* **146**, 6496–6505 (2021).
186. Chen, L. et al. High-efficiency charge transfer on SERS-active semiconducting K2Ti6O13 nanowires enables direct transition of photoinduced electrons to protein redox centers. *Biosens. Bioelectron.* **191**, 113452 (2021).
187. Pettinger, B., Schambach, P., Villagómez, C. J. & Scott, N. Tip-enhanced raman spectroscopy: near-fields acting on a few molecules. *Annu. Rev. Phys. Chem.* **63**, 379–399 (2012).
188. Lindquist, N. C., de Albuquerque, C. D. L., Sobral-Filho, R. G., Paci, I. & Brolo, A. G. High-speed imaging of surface-enhanced Raman scattering fluctuations from individual nanoparticles. *Nat. Nanotechnol.* **14**, 981–987 (2019).
189. Kim, J., Nam, S. H., Lim, D.-K. & Suh, Y. D. SERS-based particle tracking and molecular imaging in live cells: toward the monitoring of intracellular dynamics. *Nanoscale* **11**, 21724–21727 (2019).
190. Futamata, M. Surface-enhanced vibrational spectroscopy: SERS and SEIRA. *Isr. J. Chem.* **46**, 265–281 (2006).
191. Mueller, N. S. et al. Surface-enhanced Raman scattering and surface-enhanced infrared absorption by plasmon polaritons in three-dimensional nanoparticle supercrystals. *ACS Nano* **15**, 5523–5533 (2021).

Acknowledgements
This work was supported by the National Natural Science Foundation (grant nos. 21773079 (X.X.H.), 21773080 (B.Z.) and 21974054 (X.X.H.)) of P. R. China.

Author contributions
Introduction (B.Z.); Experimentation (R.S.R. and C.L.H.); Results (Y.O.); Applications (X.X.H.); Reproducibility and data deposition (X.X.H.); Limitations and optimizations (B.Z.); Outlook (B.Z.); Overview of the Primer (B.Z.).

Competing interests
The authors declare no competing interests.

Peer review information
Nature Reviews Methods Primers thanks L. He, who co-reviewed with H. Dai, and the other, anonymous, reviewer(s) for their contribution to the peer review of this work.

Publisher's note
Springer Nature remains neutral with regard to jurisdictional claims in published maps and institutional affiliations.